The Effect Of Heating Rate On The Martensite To Austenite Transformation In Iron - Nickel - Carbon Alloys.

THE EFFECT OF HEATING RATE ON THE MARTENSITE TO AUSTENITE TRANSFORMATION IN Fe-Ni-C ALLOYS

by

Charles Arthur Apple

A Dissertation

Presented to the Graduate Committee

of Lehigh University

in Candidacy for the Degree of

Doctor of Philosophy

in

Metallurgy and Materials Science

Lehigh University

1971

Approved and recommended for acceptance as a dissertation in partial fulfillment of the requirements for the degree of Doctor of Philosophy.

Aug 31, 1971
(date)

Professor in Charge

Accepted Sept. 10, 1971
(date)

Special committee directing the doctoral work of Mr. Charles A. Apple.

Chairman

Malcolm J. Roberts

David A. Thomas

Alan W. Pense

ACKNOWLEDGMENTS

The author wishes to express his sincere appreciation to his advisor, Dr. George Krauss, for his enthusiastic guidance and encouragement throughout the course of this investigation. The author is also indebted to Dr. A. W. Pense, Dr. M. J. Roberts and Dr. D. A. Thomas for their advice and service on the doctoral committee guiding this study and to Mrs. Louise Valkenburg for aid in preparing the final manuscript. The friendship of many of the faculty and staff of the Department of Metallurgy and Materials Science at Lehigh University has made the author's years in graduate school a memorable experience.

Special thanks are due to the author's wife, Linda, for her encouragement, assistance and understanding throughout the author's academic career.

TABLE OF CONTENTS

LIST OF TABLES

LIST OF FIGURES

ABSTRACT

Martensitic specimens of a series of Fe-Ni-C alloys with carbon contents of 0.004, 0.05, 0.3, and 0.6 wt pct were transformed to austenite at heating rates of 3°C/s to 28,000°C/s by resistance heating of wires. The temperatures at which the $\alpha' \rightarrow \gamma$ transformation began (A_s) and ended (A_f) were determined from thermal arrests recorded during continuous heating and structures were examined by light and electron microscopy. Mechanical properties were determined on specimens heated at 3°C/s and 1500°C/s. In the three higher-carbon alloys, A_s decreased slightly as heating rate increased while A_f initially increased by as much as 50°C with increasing heating rate. After a maximum A_f was reached, further increases in heating rate lowered A_f. The complex dependence of A_s and A_f on heating rate was associated with two different, often competing, transformation mechanisms. One mechanism is accompanied by the sharp surface tilting characteristic of a shear-type transformation and results in acicular areas of austenite with high dislocation densities. The second mechanism is thermally activated and shows only rounded surface relief. Transformation by this mechanism involves the growth of equiaxed areas of γ, apparently by short range diffusion across an incoherent interface. It is undoubtedly this thermally activated mechanism which is responsible for the large initial increase in A_f with heating rate but austenite can form by both mechanisms at low and intermediate heating rates, with

the shear mechanism eventually predominating at the higher rates. The 0.004C alloy apparently transforms only by the shear mechanism and shows no A_f variations over the entire range of heating rates. The substructures of the cycled austenites in the 0.05, 0.3, and 0.6C alloys heated at 3°C/s are significantly different from those formed at 1500°C/s due to rate-dependent tempering processes, such as carbide formation in the parent martensite, as well as transformation mechanism changes.

The yield strengths of cycled austenites of all four alloys were greatly increased compared to uncycled austenite. For example, the 0.3C uncycled austenite had a yield strength of 21 ksi, compared to 72 ksi after $\alpha' \rightarrow \gamma$ transformation at 3°C/s. Increasing the heating rate to 1500°C/s resulted in additional yield strength increases of 21, 26, and 30 ksi for the 0.05, 0.3, and 0.6C alloys, respectively, reflecting the substructural changes due to tempering and transformation mechanism differences. The same increase in heating rate had essentially no effect on the austenitic strength of the 0.004C alloy in which the transformation mechanism does not change and tempering is minimal due to the low carbon content.

Although more retained austenite was invariably present in cycled than in uncycled martensitic specimens, increases in yield strength of 10-16 ksi were obtained by cycling the three lower carbon alloys at 3°C/s. Increasing the heating rate to 1500°C/s resulted in an enhanced strengthening response only in the 0.05 and 0.3C alloys. Cyclic transformation was most beneficial to the 0.3C alloy in which

the yield strengths were 143, 159, and 167 ksi, respectively, for uncycled, 3°C/s cycled and 1500°C/s cycled martensitic specimens and the strengthening was accompanied by an increase in elongation. Cyclic transformation failed to strengthen the 0.6C martensitic specimens because of a large loss in carbon solid solution strengthening due to excessive tempering during the heating cycle.

INTRODUCTION

An increasing amount of effort is being spent in studying solid state phase transformations in order to obtain information which may be valuable in developing new alloys and methods of treatment to satisfy ever-growing demands for high-strength materials. One of the most important and interesting classes of phase transformations is the martensitic-type transformation whereby the parent lattice is converted to the product by shear and no long-range atom movements are required. Although most commonly associated with transformations which occur during cooling, the martensitic mechanism may also be operative on heating, providing the heating rate is sufficient to suppress decomposition by thermally activated processes which usually require a smaller driving force in a given material. Indeed, reversibility is one of the characteristics commonly associated with ideal martensitic-type transformations.[1]

Perhaps the most widely studied materials with respect to reversible martensitic transformations are Fe-Ni alloys.[2-6] These alloys, with Ni content adjusted so that M_s is below or only slightly above room temperature, are known to undergo both the austenite to martensite and reverse transformations martensitically over a very wide range of compositions.[2] A number of investigators have demonstrated that large increases in the strength of austenite in Fe-Ni alloys can be induced by one or more cycles of $\gamma \rightarrow \alpha' \rightarrow \gamma$ transformation. The literature on this subject up to 1962 has been reviewed in reference (4). The increase in strength due to cyclic transformation has been attributed in large part to the accumulated imperfections resulting from

the martensitic nature of both the $\gamma \rightarrow \alpha'$ and $\alpha' \rightarrow \gamma$ transformations.[6]

Some, more recent, investigations[7-10] have been concerned with obtaining even greater improvements in the strengthening response due to cyclic heat treatment through the addition of carbon to Fe-Ni base alloys with and without carbide-forming elements. These investigations dealt exclusively with the strength and structure developed by subjecting these alloys to transformation cycles under a variety of experimental conditions. Although structural similarities with martensitically reversed Fe-Ni austenite were noted[7,8] the mechanism of the transformation was not definitely established.

Although the literature cited indicates that the reverse transformation in Fe-Ni alloys can occur by a martensitic mechanism, even at moderately low heating rates, recent work[11-13] has shown that it is possible for the transformation to occur, at least partially, by a diffusion-controlled process if the heating rate is sufficiently slow (0.3°C/min for Fe-32.5 wt pct Ni).[12] No such definitive studies have been reported regarding the effect of heating rate on the martensite to austenite transformation mechanism in Fe-Ni-C alloys, although it would seem that this consideration should be of the utmost importance in deriving the maximum strengthening response from cyclic heat treatments.

There is good reason to suspect that the martensite to austenite transformation characteristics might exhibit a greater heating rate dependence in Fe-Ni-C than in Fe-Ni alloys. Examination of the A_f data reported by Hyatt and Krauss[7] for several Fe-Ni-C alloys with compositions adjusted to give a constant M_s temperature indicates that

A_f tends to increase with carbon content. These higher transformation temperatures increase the likelihood for the occurrence of a thermally activated transformation and thus the critical heating rate for austenite formation by a martensitic mechanism may be expected to increase.

A number of precedents exist in the literature for an investigation of the effects of rate of temperature change on the transformation mechanisms of ferrous materials. The most common example of this involves the effect of cooling rate on the decomposition of austenite in steel, in which several transformation mechanisms and a variety of transformation products are possible. A large amount of work in the last decade has established that transformations in other, less complicated ferrous materials can be influenced by cooling rate. The mechanism of the $\gamma \rightarrow \alpha$ transformation in pure iron and dilute Fe-C alloys has been found [14-16] to change from a thermally activated process to a martensitic one if a critical cooling rate is exceeded. This critical rate (and the M_s temperature) decreases extremely rapidly as carbon content is increased. [14] A similar effect has been noted in several substitutional alloys. [16-18]

The $\alpha' \rightarrow \gamma$ transformation usually occurs at temperatures high enough so that carbon diffusion and resultant carbide precipitation are appreciable. Carbide particles have been observed in both the martensite and austenite of Fe-Ni-C alloys subjected to partial and complete $\alpha' \rightarrow \gamma$ transformation at heating rates of several hundred °C/min [7] and 1000°C/s. [9] Other observers have reported the presence of alloy carbide particles produced by subjecting Fe-Ni-V-C [8] and

Fe-Ni-Mo-C[10] alloys to the martensite to austenite transformation at various heating rates.

It has not yet been established to what degree the presence of highly mobile carbon atoms and carbide particles affect the kinetics of the reverse transformation. However, in the case of the austenite to martensite transformation, variations in M_s with cooling rate have been reported for 52100 steel[19] and Fe-0.5C.[20] This effect has been attributed to changes in the shear strength of the parent austenite due to carbon segregation prior to $\gamma \rightarrow \alpha'$ transformation. Also, in an Fe-Ni-Al alloy, Hornbogen and Meyer[21] have shown that it is possible to depress M_s by as much as 200°C if coherent Ni_3Al particles are precipitated in the matrix prior to transformation. In a more recent investigation[22] incoherent phosphide particles in austenite have been observed to inhibit the formation of martensite, causing local areas of incomplete transformation.

Since it is to be expected that the carbide morphology in the parent martensite of Fe-Ni-C alloys would depend upon the heating rate, so also might the transformation kinetics of the $\alpha' \rightarrow \gamma$ transformation. Haworth and Parr,[23] using a thermal arrest technique, have reported the A_{c_3} temperature of Armco iron heated from room temperature to be practically independent of heating rate while that for the same material held at 800°C prior to transformation increased with heating rate. It was suggested that the rate independence in the former case indicated the occurence of a martensitic-type mechanism and that the latter results indicated a diffusion-controlled transformation, the mechanism depending on the distribution of carbon in

the iron.

Albutt and Garber[24] have investigated the effect of heating rates up to 2000°C/s on the austenitizing behavior of pure iron and a low-carbon mild steel, using dilatometry to determine the transformation start and finish temperatures. They also provided evidence for a "diffusionless" $\alpha \rightarrow \gamma$ transformation according to the same criterion used by Haworth and Parr.[23] It was also concluded that the rate at which the diffusionless transformation becomes dominant is dependent upon the carbide morphology.

One of the difficulties commonly encountered in defining transformation mechanisms which occur on heating lies in establishing criteria that differentiate a martensitic mechanism from those which are thermally activated. Kinetic criteria such as the degree of dependence of transformation temperatures on heating rate, as used in some of the previously-mentioned work,[23,24] are not conclusive.[1,25] Although in most cases martensitic transformation temperatures are not a function of cooling or heating rate, the same behavior has been reported for the transformation-start temperatures of a variety of materials transforming by the massive mechanism.[14,17,26] Bharucha et al.[27] used thermionic emission microscopy to monitor the motion of the $\alpha \rightarrow \gamma$ interface during the heating and cooling of high purity iron and dilute Fe-Ni and Fe-Mo alloys. These authors, adopting the criterion of Eichen and Spretnak,[28] suggested that the observed discontinuous motion of the interface indicated a martensitic mechanism on both heating and cooling at unspecified rates. This criterion has met with severe criticism. (See the written discussion accompany-

ing reference (28).) There are other conflicts regarding morphological, habit plane and orientation relation criteria.[29]

The most widely-accepted criterion distinguishing a martensitic-type transformation is the occurrence of sharp tilt surface relief features characteristic of an invariant-plane strain. This criterion has recently been reviewed extensively by Clark and Wayman,[29] and the case for it greatly strengthened by their conclusion that, in general, those transformations which display an invariant-plane strain relief effect also exhibit the other crystallographic characteristics of a martensitic transformation. Any investigation involving determination of the transformation mechanism should be designed, if possible, to make use of surface relief criteria.

PURPOSE

The purpose of this investigation is to establish the effect of heating rate upon the nature of the martensite to austenite transformation in a series of Fe-Ni-C alloys. The effect of variations in heating rate upon carbide distributions and other structural features of the austenite formed by a complete cycle of $\gamma \rightarrow \alpha' \rightarrow \gamma$ transformation will also be studied. The mechanical properties of cycled specimens will be measured and related to variations in the structural features produced by changes in heating rate. Such information will be useful in deriving the optimum strengthening response from cyclic heat treatment in these alloys.

The temperature of the start and finish of the $\alpha' \rightarrow \gamma$ transformation as a function of heating rate will be determined by thermal arrest methods and should provide information regarding the nature of the transformation on continuous heating. Particular emphasis will be placed on determining the transformation mechanism by surface relief, kinetic, microstructural, and fine structural observations.

EXPERIMENTAL PROCEDURE

A. Materials

A series of four Fe-Ni base alloys with carbon varying from 0.004 wt pct to 0.6 wt pct was used. The nickel content was balanced against the carbon so that the M_s temperatures would be below room temperature but high enough to result in predominantly martensitic structures when cooled to -196°C. The exact chemical analyses of the alloys are presented in Table I. The alloys, which will hereafter be designated by their carbon contents, were all prepared by vacuum melting electrolytic iron and nickel and, except for the 0.004C alloy, spectrographic carbon rod. The three higher carbon alloys were received in the form of hot-forged bars approximately 3/4 in. in diameter while the 0.004C alloy had been hot rolled to 5/8 in. square cross-section bars.

The bars were cut into 10 in. lengths and machined to 1/2 in. diameter before being swaged to 0.095 in. diameter in 13 steps. The 0.6C specimens required an intermediate annealing treatment after passing through the 0.156 in. swaging dies. This was done at 1000°C for 1 hour with the specimens in evacuated vycor capsules. The 0.095 in. diameter specimens were cut into 4 in. lengths, vacuum encapsulated in vycor tubes, and homogenized at 1100°C for 2 hours. Immediately after removal from the furnace, the capsules were broken in water in order to minimize any carbon segregation effects on cooling. This treatment resulted in completely austenitic structures, the ASTM grain sizes of which were determined by comparison with the grain size reticle on a Balphot II metallograph and are reported in Table II.

Martensite was formed by cooling to -196°C in liquid nitrogen for 30 minutes immediately preceding the heating cycle in order to minimize and standardize the room temperature aging known to occur in Fe-Ni-C martensites.[30]

B. Heating Techniques

1. Apparatus:

A wide range of heating rates was achieved by construction of a direct resistance heating apparatus adapted from that described by Haworth and Parr.[23] This apparatus is shown schematically in Figure 1 and the physical configuration is shown in Figure 2(a). The power source consisted of a parallel arrangement of five 12 volt batteries kept at maximum potential by a trickle charger. The remainder of the unit consisted mainly of solenoid switches controlled by electronic timers through which the duration of the heating cycle and hence the maximum temperatures were controlled. It was possible to either heat at slow rates or hold at temperature by activation of the circuit which applied R_2, a 2 x 2 in. carbon block rheostat, in series with the specimen. The specimens, except those prepared for surface relief studies, were mounted in a holder which consisted of two double-jawed clamps separated by a strip of transite. The separation of the clamps was variable from 1/2 in. to 4 in., providing a second method of varying heating rate. After the timed heating cycle and a controlled delay time, the specimen could be water quenched by the automatic activation of an AC solenoid which swung the specimen, still mounted in its holder, into a dish of water. This quenching apparatus is

shown in Figure 2(b).

The direct discharge of the five batteries through the 0.095 in. diameter martensitic specimens resulted in a heating rate of between 1400 and 1600°C/s, depending on the alloy, when the distance between contact points was 2 1/4 in. Rates as high as 28,000°C/s were obtained by reducing the contact length to 3/4 in. and reducing specimen diameter to 0.045 in. Small diameter specimens were produced by rolling in a chemical polishing solution of 16 H_2O_2-$3H_2O$-1HF.

2. Temperature Measurements:

Because of the rapid heating rates realized with the above apparatus, it was necessary to take thermocouple response time into account. Fine-wire intrinsic thermocouples are known to be superior in this respect.[31] However a problem arises with the use of a standard two-element intrinsic thermocouple in that, due to the large current used to heat the specimen, a non-thermal emf is generated between the two thermcouple junctions. This non-thermal emf may be many times greater than the thermal emf unless the two components are joined to the specimen exactly at points of equi-potential, a condition which would be extremely difficult to satisfy. For this reason, a modification of the thermocouple, called a "thermotrio"[23,32,33] was employed. This arrangement consisted of two 0.003 in. diameter chromel wires on each side of an alumel wire of the same diameter. The three wires were welded approximately 0.020 in. apart near the center of the specimen. Welding the small wires to the specimen was facilitated by the construction of a spot welding device similar to that used by Karlyn.[34] The spot welder is shown in Figure 3. Light electrode

pressure and low power were used to minimize the heat-affected zone in the specimen. The two outer thermocouple wires (chromel) were joined across a variable resistor. Momentary current pulses small enough to avoid significant heating were applied to the specimen through push-button switch S6 and the emf between the center (alumel) element and the wiper arm of the resistor was observed by noting the deflection of a light galvanometer. The resistor was adjusted until no discontinuity in emf was observed when a current pulse was applied. The condition for balance of the thermotrio is given in the Appendix.

For rates of 500°C/s and above, the output of the thermotrio as a function of time during the heating cycle was recorded by photographing the trace of a Tektronix 502A Oscilloscope triggered automatically when the heat cycle started. A Honeywell strip chart recorder with a full scale response time of 1/2 sec. was adequate at the lower heating rates. A standard cold junction correction of +1.0 mv was applied. Any error due to improper thermotrio balancing could be detected by a discontinuity in the mv vs. time curves at the beginning and end of the heating period. This error could then be added or subtracted from the reading taken. Typical curves of temperature vs. time obtained from the recorder and from the oscilloscope are shown in Figure 4(a) and (b), respectively. The good reproducibility possible at the higher rates is indicated by the three separate curves of Figure 4(b).

C. Determination of A_s and A_f Temperatures

The temperatures corresponding to the onset (A_s)* and completion (A_f)* of the $\alpha' \rightarrow \gamma$ transformation were determined from the temperatures marking the beginning and end of the thermal arrest due to the endothermic transformation on the otherwise relatively linear T-t curves. The thermal arrest method has been used by a number of investigators [14,17,23,35-37] to determine transformation temperatures. Figure 4(a) illustrates the method used. At rates lower than about 3°C/s, non-linearity of the T-t curves became pronounced, therefore no A_s-A_f data are available below this rate.

Results of analyses of a number of T-t curves at a given heating rate were averaged in order to arrive at accurate values for A_s and A_f. Because of the relatively small scale of the T-t trace obtained from the oscilloscope, each separate trace was analyzed 5 times and these results were averaged in order to minimize the error arising from judgement of the points of deviation from linearity.

D. Surface Relief Studies

Specimens to be used for surface relief studies were made from 1 1/2 - 2 in. lengths of 0.095 in. diameter martensitic samples which were mounted in cold-mounting plastic, ground to a semi-circular cross

---

*Although the terms "A_s" and "A_f" were originally intended to imply an analogy to M_s and M_f associated with martensitic transformations on cooling, A_s and A_f will be used here for convenience to denote the temperature at which the $\alpha' \rightarrow \gamma$ transformation begins and ends, respectively, on continuous heating, regardless of the actual transformation mechanism.

section and polished through Linde B abrasive. The specimens were then clamped into copper terminals mounted on a transite strip and inserted into a 35 mm I.D. quartz tube. Copper contacts extending through rubber stoppers at each end of the tube provided electrical contact. This setup is pictured in Figure 5. The system was flushed with argon for several minutes before high purity dry hydrogen (dew point better than -60°C) was passed through the tube and burned at one end. It was under this small positive pressure of hydrogen that the complete heating and cooling cycles were applied. There were no provisions for a rapid quench of the surface relief specimens.

Examination of the surface was conducted with a Zeiss Phase Contrast microscope. Areas of interest were marked with a diamond pyramid indentor on a Tukon Microhardness Tester. Microstructural features corresponding to relief features were brought out by etching over the relief with 20 g $CuSO_4$, 100 ml HCl, 100 ml H_2O, 200 ml ethanol for the 0.004 and 0.05C alloys and 1 pct nital for the 0.3 and 0.6C alloys.

E. Electron Microscopy

Thin foils for transmission electron microscopy were prepared from 0.015 in. thick discs sliced from the 0.095 in. diameter specimens with a Servomet EDM machine or from rectangular longitudinal sections ground from smaller-diameter specimens. Samples were then inserted into a hole of corresponding size in a 1/2 in. square piece of 0.005 in. thick shim stock held to a bakelite block with double stick tape and ground in several steps through #600 wetpaper to 0.005 in. The EDM unit with a slightly rounded copper electrode was used to produce an indentation

approximately 0.001 in. deep on each side of the disc. The specimen was then electropolished in a jet thinning apparatus with an electrolyte of 798 ml acetic acid, 150 g CrO_3 and 42 g H_2O at 20 volts.

Carbon extraction replicas of the 0.3C alloy were prepared from cycled martensitic specimens by evaporating a layer of carbon approximately 300Å thick on surfaces which had been polished and lightly etched in 1 pct nital. After being scribed into suitably sized grids, the carbon replicas were stripped in the etching solution. Thin foils and carbon extraction replicas were examined in an RCA EMU3G electron microscope operating at 100 kv.

F. Mechanical Testing

Specimens for tensile testing were prepared from the 0.095 in. diameter samples. Experiments in which two thermotrios were attached at different points of a specimen indicated that at heating rates of 1500°C/s no significant thermal gradient was present within 1 in. of the center. Specimens heated 2.5°C/s to 450°C at the center showed that differences in temperature of up to $\pm$12°C could occur at points 3/4 in. from the center. For this reason, it was decided to restrict the gage length of tensile specimens to 3/4 in. (3/8 in. on each side of center).

Figure 6 shows a tensile sample at various stages of its preparation. The ends of the samples were coated with lacquer, leaving a 3/4 in. gage length at the center. The gage length was then reduced to 0.070 $\pm$ 0.0005 in. by rolling in a solution of $16H_2O_2$, $3H_2O$, 1HF. Rounded shoulders were obtained by scraping back the lacquer at least once during the process.

Tensile testing was done on an Instron unit at a crosshead speed of 0.02 in. per min. Strip tensile grips were used and, to aid axial alignment of the specimen, steel inserts with serrated grooves were fabricated. All specimens to be tested in the martensitic condition were stored in the austenitic condition and cooled to -196°C for 30 minutes in liquid nitrogen, from which they were removed and warmed to room temperature no more than 5 min. before testing. Elongation was monitored with a 1/2 in. strain gage extensometer. At least three specimens were tested in each condition and the results were averaged.

G. Standard Heating Cycles

Specimens of each alloy to be used for tensile testing or for structural observations after a complete transformation cycle were subjected to treatments which involved heating martensitic specimens at 3°C/s or 1500°C/s to a predetermined reversal temperature somewhat above A_f. Specimens heated 3°C/s were quenched by manual activation of the quench solenoid as soon as the desired temperature was reached. Reversal temperatures for each alloy heated 1500°C/s were controlled by standard settings on the heat cycle timer and a short delay time of about 0.15 sec was applied before the quench solenoid was automatically activated. The average reversal temperatures for specimens of each alloy heated 3°C/s and 1500°C/s along with the A_f temperatures determined at those rates are given in Table III.

RESULTS AND DISCUSSION

A. Transformation Temperatures

The thermal arrest data are presented in Figures 7-11 where the A_s and A_f temperatures of the four alloys are shown as functions of heating rate. Each data point represents the average of the data taken from tests performed on as many as 21 but no fewer than 4 specimens. The standard deviation of the data is indicated. The A_s data for the two lower-carbon alloys are incomplete at low heating rates owing to the absence of a discernable change in slope of the temperature vs. time curves below the A_f temperatures. This suggests that the lower C (higher Ni) alloys have a lower enthalpy associated with the $\alpha' \rightarrow \gamma$ transformation than do the higher carbon (lower Ni) alloys. Although no enthalpy data were found for the Fe-Ni-C system, the calculations of Kaufman and Cohen[25] and the data of Scheil and Normann[38] show a decreasing (positive) enthalpy with increasing Ni content above 15 at. pct in Fe-Ni alloys. Also, since one might expect the driving force for transformation to depend upon the shear strength of the parent in a martensitic transformation, the higher-carbon alloys would be expected to require a higher driving force for transformation and a higher enthalpy.[25] The reason that the A_s temperature becomes more well-defined on the T-t curves of these lower-carbon alloys at higher heating rates is undoubtedly due to the shorter time available for radiation heat losses and consequently the much more nearly adiabatic nature of the system.

In general, the return to a constant slope of the temperature-time curve which was taken to denote the A_f temperature was much more well-

defined than the deviation of the trace from a constant rate which marked the A_s temperature, an indication that the rate of the martensite to austenite transformation may be higher in the high-temperature range near the A_f than at temperatures close to A_s. The better definition of A_f could also be enhanced by the steeper slopes of the T-t curves at temperatures above A_f.

The A_f temperature, 368°C, for the 0.004 C alloy as shown in Figure 7 is practically independent of heating rate over the entire range of rates. The small amount of data available for A_s in this alloy is insufficient to indicate any trend. The martensitic nature of austenite formation in an almost identical alloy (Fe-32.5 wt pct Ni) has been definitely established at heating rates as low as 10°C/min. (12) by crystallographic and surface relief criteria. The independence of the A_f data with heating rate for the 0.004C alloy is indicative of an athermal transformation and suggests the mechanism of austenite formation remains martensitic over the given range of heating rates.

The three higher-carbon alloys all exhibit changes in transformation temperatures with heating rate. The A_f temperature of the 0.05C alloy, Figure 8, increases from about 425°C at 3°C/s to 443°C at 160°C/s and then appears to decrease again at higher heating rates. The available data for A_s indicate a decreasing trend with increasing heating rate, although the scatter in the data becomes considerable at high rates of heating.

The 0.3C and 0.6C alloys, Figures 9 and 10, respectively, showed more pronounced increases in A_f with heating rate in the lower range before apparently decreasing slightly at higher rates. The A_f temper-

ature of the 0.3C alloy increased from 493°C at 3°C/s to about 540°C at 1100°C/s while that for the 0.6C alloy increased from 515°C at 2.5°C/s to 553°C at 180°C/s. In both cases the A_s temperatures appeared to decrease slightly with heating rate, possibly leveling off in the range of higher heating rates. The initial increase in A_f with heating rate in three higher-carbon alloys suggests that at least part of the martensite to austenite transformation in these alloys occurs by a thermally activated mechanism.

The A_f temperatures determined for the four alloys are shown in relation to each other in Figure 11. It can be seen that the transformation temperatures in general increase with the alloy carbon content. Although the alloy compositions were such that Ni content decreased as carbon content increased, in the three higher carbon alloys this was done to produce equivalent M_s temperatures and so it appears that the driving force necessary for the $\alpha' \rightarrow \gamma$ transformation increases with carbon content. This could be due to the large strengthening effect due to carbon,[30] increasing the resistance of the parent martensite to a shear-type transformation. On the other hand, carbon in solution has a relatively small effect on austenite strength so that M_s may be made relatively constant by balancing the C and Ni contents.

B. Optical Metallography

The shapes of the transformation temperature vs. heating rate curves for the 0.05, 0.3, and 0.6C alloys are complex and no attempt to completely interpret them can be made without further evidence

regarding the nature of the martensite to austenite transformation in these alloys. For this reason, a study of relief effects and morphological features produced under a wide range of conditions was undertaken. Figure 12 shows the original martensitic structures of the four alloys after cooling in liquid nitrogen. All alloys display the twinned plates characteristic of high Ni, low M_s martensite. Midribs and deformation twins are clearly visible in the larger plates and a large range of martensitic plate sizes is present, especially in the three higher-C alloys. Significant amounts of retained austenite are present, 22.7%, 8.6%, 10.7%, and 15.4% for the four alloys in order of increasing carbon.

The relief effects observed when a prepolished specimen of the 0.05C alloy was completely transformed to austenite at 3°C/s and 3000°C/s are shown in Figures 13(a) and 13(b), respectively. Definite sharp tilt relief effects are in evidence in both cases, but there are subtle differences between the two structures. The specimen heated at 3°C/s shows a number of areas which are smooth or where only surface rumpling is observed. For example, the large martensite plate near the center of Figure 13(a) (see arrow) shows the sharp relief effects characteristic of a shear-type transformation in its middle while part of the outer edge is quite flat.

Further evidence of a difference in transformation mechanism with heating rate in the 0.05C alloy was obtained by examining specimens partially transformed by heating to a temperature between A_s and A_f. Figure 14(a) shows a prepolished surface of the 0.05C alloy subjected to partial transformation at 3°C/s and the same area after etching in

14(b). Areas of relatively sharp relief as in the lower left-hand corner of Figure 14(a) correspond to small martensite plates which have almost completely transformed by shear to austenite. The large areas of relative smoothness in 14(a) can be seen in 14(b) to consist of larger martensite plates which have partially transformed to austenite by deterioration from the edges. In this case the areas that have transformed show no sharp relief effects although the newly-formed austenite has in some cases penetrated into the midrib region as shown in Figure 14(b) and its interface with the parent martensite is generally curved, as is often characteristic of a thermally activated mechanism. These observations suggest that the transformation in the 0.05C alloy occurs by two distinctly different mechanisms at the lower heating rates. Further evidence for the dual nature of the transformation can be seen in the morphological features of the partly reversed structure in Figure 15(a).

Figure 16 shows a relief-microstructure pair of micrographs from an area of the 0.05C alloy partially transformed at 3000°C/s. The sharp, angular relief features just to the lower left of the hardness indentation are seen to correspond to long plates of austenite that fragment even the larger martensite plates at this stage of transformation. Although this specimen was cooled relatively slowly from the partial reversal temperature, little evidence for a transformation other than by a shear-type mechanism is present. The microstructure of a specimen which was water cooled after partial transformation, Figure 15(b), also confirms that the increase in heating rate by a factor of 10^3 resulted in an increase in the degree of transformation which

occurred martensitically.

Relief effects on specimens of the 0.3C and 0.6C alloys were generally smaller and harder to distinguish. Figure 17 shows a relief-structure pair from the 0.3C alloy reversed at 3°C/s. As in the 0.05C alloy at this heating rate many of the smaller plates appear to have transformed by a shear mechanism as shown by the surface tilting surrounding the large, smooth martensite plates in Figure 17(a). Also, as in the 0.05C alloy, the dual mechanism of the transformation is affirmed by the two drastically different types of surface effects and corresponding morphological features in Figure 17(b). The rumpled or bulged area marked by the large arrow in Figure 17 shows only the relief attributable to a volume change[29] and corresponds to a newly-formed area of austenite in the center of a martensite plate. The lack of tilt-type surface relief and the curved boundary morphology of this area provide strong evidence that austenite has formed by a thermally activated mechanism. The small arrows indicate shear relief effects, seen in Figure 17(b) to correspond to straight-sided austenite areas at the edge of a large martensite plate. Figure 18(a) shows another example of the transformation morphology of the 0.3C alloy partially reversed to 3°C/s. The thermally activated disintegration of large martensite plates in the latter stages of transformation is quite evident.

Little additional information was obtained from relief-structure pairs of the higher-carbon alloys heated at high rates. The relief features observed after partial transformation at 3600°C/s were remarkably similar to those obtained at 3°C/s. One explanation for this is that a large part of the transformation observed after high-rate

heating may have actually taken place during the period when the partly transformed relief specimens were cooling at a relatively slow rate. Because of this possibility, the discussion of the structure of rapidly transformed specimens of the 0.3C and 0.6C alloys is limited to the morphological features of non-relief specimens in which an immediate rapid quench was possible.

Figure 18(b) clearly shows that the $\alpha' \rightarrow \gamma$ transformation of the 0.3C alloy at 1450°C/s occurs largely by the formation of plates of austenite along certain crystallographic directions within the original martensite plates. In most cases these austenite segments terminate at the martensite midrib. The shape and well-defined crystallographic orientation of the plates suggests that the austenite formation has occurred by a shear-type transformation mechanism. Comparison of Figure 18(a) with Figure 18(b) indicates that the proportion of transformation by a shear-type mechanism increases with heating rate in the 0.3C alloy as was observed in the 0.05C alloy.

The thermally activated $\alpha' \rightarrow \gamma$ transformation occurred to the largest extent in slowly heated specimens of the 0.6C alloy. A 3°C/s partially reversed relief-structure pair is shown in Figure 19. Some sharp relief is present but also quite evident are the rounded relief features which are seen in Figure 19(b) to correspond to newly-formed austenitic areas with curved boundaries.

Figure 20 shows a sequence of structures produced by heating the 0.6C alloy at 3°C/s to various temperatures between A_s and A_f followed by an immediate water quench. The thermally activated transformation is most evident in the larger martensite plates at 504°C, Figure 20(b),

although it can also be seen in smaller plates. At 508°C, the areas of thermally activated transformation have impinged and have nearly consumed the large martensite plate in Figure 20(c). On heating to 513°C, Figure 20(d), only scattered remnants of martensite remain. This sequence also confirms independently the validity of the thermal arrest method of transformation temperature determination by which the A_s and A_f were determined to be 498 $\pm$4°C and 515 $\pm$1.3°C, respectively, at a heating rate of 2.5°C/s.

Figure 21(a) shows more clearly the nature of the interfaces associated with the thermally activated transformation in the slowly-heated 0.6C alloy. Although in some cases the transformation interface apparently coincides with deformation twins in the martensite, the retarding effect of these features appears to be only temporary and the generally curved, irregular boundaries are indicative of an incoherent interface. A different morphology of the newly-formed austenite was observed after partial transformation at 1570°C/s and immediate quenching, as shown in Figure 21(b). The shape of the newly-formed austenite areas indicates that the proportion of transformation by a shear mechanism is greater at the higher heating rates, as was also observed in the 0.05 and 0.3C alloys.

C. Electron Microscopy

Thin foils were examined in order to determine the effect of heating rate upon carbide morphology and other fine structural features. Figure 22 shows the appearance of the as-quenched martensite in the 0.3C alloy. The structure displays the general "mottling" characteristic of Fe-Ni-C martensite aged at room temperature.[39] The absence of well-developed carbide particles attests to the ability of the dimpling and thinning techniques to produce foils with a minimum of overheating. Figure 23 shows the carbide distribution produced in a martensitic specimen of the 0.3C alloy which was tempered by heating at 3°C/s to 400°C (about 50°C below A_s for this heating rate) before being quenched in water. This treatment has produced well-developed planar carbide particles which appear quite similar to those identified as cementite by Tekin and Kelly[39] and Wells.[40] Specimens heated to 435°C at 1500°C/s and immediately quenched appeared to contain two different carbide morphologies. Figure 24(a) shows carbides similar in appearance but generally somewhat smaller and more uniformly distributed than the cementite observed in the slowly heated specimens. Occasionally carbide morphologies such as that shown in Figure 24(b) were observed. These precipitates appear ribbon-like in the thin foils and are similar in morphology to those observed in Fe-Ni-C alloys tempered below 200°C and identified as ε-carbide.[39,40] However, single surface trace analyses of carbides in a number of different areas of martensitic foils tempered by heating at 1500°C/s failed in all cases to show consistency with the $(100)_\alpha$ habit known to exist for ε-carbide.[39,40] Many of the traces were consistent with either the

$(110)_\alpha$ or $(211)_\alpha$ habit observed for cementite in untwinned and twinned areas, respectively, but the scatter in the data was considerable, making a positive correlation impossible.

Thin foils of the 0.3C alloy subjected to partial martensite to austenite transformation at slow and at rapid heating rates were also examined in order to determine the fine structure of the momentarily co-existing martensite and reversed austenite. Figure 25(a) shows two areas of austenite, identified by electron diffraction, in a 0.3C specimen which was partially reversed at 3°C/s. Because of the presence of carbide particles, the areas are undoubtedly newly-formed from tempered martensite rather than areas of the original retained austenite. The equiaxed morphology of the areas suggests that the new austenite developed as the result of a thermally activated process. The orientation and size of the carbide particles within these areas is similar to those in the surrounding martensite, indicating that the operative transformation mechanism did not require solution of the particles in advance of the interface. Another partially reversed area resulting from slow heating is shown in Figure 25(b). The long segment dividing the figure diagonally was shown by combined electron diffraction and dark field techniques to be martensite and that below it was identified as austenite. Note the dense line of carbides across the boundary, extending into both phases and apparently obstructing the progress of the expanding phase boundary. The dislocation density of the austenite in both cases appears to be low although some of the dislocations may not be in contrast.

Figure 26 shows two examples of the 0.3C alloy partially reversed at 1500°C/s. Figure 26(a) shows a single martensite plate (as judged from the similar carbide orientations in each segment) which has been fragmented into a number of alternate acicular areas of martensite and austenite of the same orientation as verified by electron diffraction and dark field illumination of the two phases. At this stage of the transformation none of the rather large carbides seen in the martensite are detectable in the austenite. This could indicate that at the high heating rates the areas devoid of carbides transform first, the areas containing carbides requiring a larger driving force. Figure 26 (b) shows a larger area of austenite and its interface with the martensite. Comparison of Figure 26 with Figure 25 indicates that the austenite formed at higher heating rates contains a considerably higher defect density, an observation verified by electron micrographs of fully austenitized samples as discussed in a later paragraph.

Due to the dual transformation mechanism, austenite formed by heating the 0.3C alloy at 3°C/s varied widely in appearance. Figure 27 shows two examples from the same foil. The difference in fine structure is striking. Large cementite particles are seen in both cases but the austenitic area in Figure 26(b) has a much higher dislocation density. Rapidly heated foils of the same alloy had a much more fragmented substructure as shown in Figure 28. In the case of the rapidly-heated specimens of the 0.3C only limited definite evidence is seen of the rod or lath-shaped carbides (see arrows, Figure 28) which were such an integral part of the parent structure. It is possible that the highly fragmented defect structure seen in foils of the rapidly transformed austen-

ite could obscure small carbides, but carbon extraction replicas prepared from cycled martensitic specimens of the 0.3C alloy heated at 1500°C/s, Figure 29(a), also failed to reveal carbide particles while those prepared from slowly heated specimens, Figure 29(b), showed many particles.

When the 0.3C alloy was tempered by heating to 400°C at 3°C/s to produce the structure shown in Figure 23, and then austenitized at 1500°C/s, some of the larger cementite particles were retained in the cycled austenitic structure. Figure 30 shows the austenitic structure developed by such a treatment. Except for the presence of occasional rows of closely-spaced large carbides in the pretempered specimens as in the slowly austenitized specimens (see Figure 27(b)), the appearance of the cycled austenite was quite similar to that noted in conventional specimens austenitized at 1500°C/s. However, in contrast to Figure 27 (b) the carbides shown in Figure 30 have apparently acted to retard the transformation interface, thus delineating the boundary between two newly-formed austenitic areas.

Cycled austenitic specimens of the 0.6C alloy contained large carbide particles after transformation during heating at both 3°C/s, Figure 31, and 1500°C/s, Figure 32. The 0.6C specimen heated at the higher rate had a more uniformly dense dislocation substructure and, in addition to the large particles, appears to contain a large number of much finer spherical particles.

A limited amount of transmission electron microscopy of the 0.05C alloy revealed somewhat similar substructures in austenite cycled at 3°C/s and at 1500°C/s, Figure 33(a) and (b), respectively. Although

both structures appear to contain some very small particles, these are much more evident in the rapidly-heated specimens, even though the fine structure produced by rapid heating appears to be somewhat more fragmented.

D. Interpretation of A_s and A_f vs. Heating Rate Results

In view of the results presented in the preceding section, it now becomes possible to arrive at a logical explanation of some of the features of the A_s and A_f vs. heating rate curves. Although considerable evidence was found for a shear mechanism, the $\alpha' \rightarrow \gamma$ transformation in the 0.05, 0.3 and 0.6 carbon alloys occurs to some extent by a thermally activated process at the lower heating rates. The proportion of transformation by the martensitic mechanism increases with heating rate but at the lower heating rates where there is a considerable thermally activated component, A_f should increase with heating rate. It should be noted that when both mechanisms are observed to occur at a given heating rate, the relative amount of thermally activated transformation should increase with the temperature because of increasing driving force and increasing thermal activation. When the heating rate is such that the thermally activated component is suppressed, the resultant superheating provides the necessary driving force to allow the later stages of transformation to be dominated by the martensitic component and the A_f temperature should become relatively constant, as would be expected for an athermal transformation. However, for the three higher-carbon alloys the A_f reached an apparent maximum and then began to decrease in the range of heating rates where the shear transformation predominates. This may be associated with a temperature and time-dependent phenomenon which tends to suppress the martensitic-type transformation at lower rates but would have less effect as heating rate increased. The fact that the martensitic A_f temperature of the lowest carbon alloy showed essentially no variation with heating rate suggests

that the retardation of the shear-type component is associated with the presence of carbon. One way in which carbon could have a stabilizing effect on the shear transformation is by inhibition of nucleation due to carbon segregation at potential nucleation sites as proposed by Kinsman[41] to explain thermal stabilization of the $\gamma \rightarrow \alpha'$ transformation in Fe-Ni-C alloys. It is also possible that carbide precipitation in the martensite could limit the growth of shear plates and so retard the martensitic component. Thus the shape of the A_f vs. heating rate curves can be explained in terms of a dual transformation mechanism at the lower rates and a predominantly martensitic-type transformation with decreasing stabilization at the higher rates.

The general decrease in the A_s temperature with increasing heating rate noted in the three higher-carbon alloys also indicates that stabilization of the shear component of transformation occurs at the lower rates. In order to demonstrate the stabilizing effect of tempering processes occurring in the parent martensite, 12 specimens of the 0.3C alloy were pretempered by heating to 400°C at 3°C/s prior to being austenitized at 1500°C/s, a rate at which much of the transformation in the early stages occurs by shear, as shown in Figure 18(b) for example. The A_s temperature of the pretempered specimens at 1500°C/s was found to be 468 $\pm$8°C, significantly above the A_s value of 436 $\pm$11°C determined for the standard specimens heated at the same rate. Thus A_s at 1500°C/s exhibits considerable dependence upon prior martensitic condition and may be influenced by such heating rate-dependent tempering phenomena as carbide formation, carbon segregation, matrix composition changes and recovery effects.

In contrast to the A_s, the A_f temperature of the pretempered-1500°C/s reversed 0.3C specimens at 537 ±5°C was close to the A_f of 536 ±9°C noted for untempered specimens austenitized at the same rate. This similarity in A_f may be due to thermally activated completion of the $\alpha' \rightarrow \gamma$ transformation despite the observation that in this 0.3C alloy much of the transformation at 1500°C/s involves shear.

A simplified view of the model proposed to explain the observed dependence of A_s and A_f on heating rate is presented in Figure 34 where hypothetical A_s and A_f temperatures for transformation by purely martensitic (M) and purely thermally activated (TA) mechanisms are shown as dotted lines. It must be emphasized that Figure 34 is merely a schematic representation; the shape of the A_s(TA) and A_f(TA) vs. heating rate curves, arbitrarily shown as diverging straight lines, would probably be more complex. It is assumed that a reduced degree of stabilization would cause A_s(M) and A_f(M) to decrease with increasing heating rate within a certain range in a manner analogous to the behavior of M_s vs. heating rate reported for several steels.[19,20] The actual A_s or A_f temperature (solid lines) at a given heating rate should be due to that mechanism by which the transformation can begin or can end respectively, at the lower temperature. When the transformation temperature ranges for the two alternate mechanisms overlap at a given heating rate, a mixed transformation may occur.

For the example shown in Figure 34, A_s(M) lies below A_s(TA) at all heating rates, therefore A_s will closely follow A_s(M) over the entire range. At the lower rates, A_f(M) is much higher than A_f(TA) so that a large part of the transformation will take place by the thermally

activated mechanism and A_f will lie close to $A_f(TA)$. At higher heating rates, A_f follows $A_f(M)$ when the latter becomes lower than $A_f(TA)$.

The above example illustrates how the general shapes of the A_s and A_f vs. heating rate curves may be rationalized in terms of a mixed transformation mechanism. Figure 34 represents only one case which qualitatively explains the trends observed for the 0.05C, 0.3C, and 0.6C alloys. The actual positions of specific features on each curve depend upon the separate behaviors of the two mechanisms with heating rate and alloy composition and on the proportion of austenite formation by each mechanism at a given heating rate.

E. The Nature of the Thermally Activated Transformation

It has been established that the martensite to austenite transformation in the three higher-carbon alloys occurs by two competing mechanisms at the lower heating rates. One mechanism is martensitic, involving the cooperative movement of groups of atoms over distances less than one atomic spacing. This mechanism is responsible for the sharp tilt relief effects noted to some degree in all specimens examined. The second mechanism has been shown, by its effect on the A_f temperature and eventual suppression at rapid heating rates, to be thermally activated. The austenitic areas formed by this mode of transformation are equiaxed and generally display curved boundaries in contrast to the straight-sided acicular areas formed by the martensitic mechanism. Only rounded surface relief due to a volume contraction accompanies the latter mechanism.

Evidence for thermally activated isothermal $\alpha' \rightarrow \gamma$ transformation is demonstrated in Figure 35 where the structure obtained by heating the 0.6C alloy to 509°C and immediately quenching, Figure 35(a), is compared to the structure obtained by heating to 504°C and varying the temperature approximately sinusoidally between 500 and 508°C for 70 seconds, Figure 35(b). Note that the transformation, although only partially complete in the larger martensite plates of the immediately quenched sample, has almost completely consumed the larger plates of the "isothermally" held specimen.

The actual nature of the thermally activated component of transformation remains somewhat uncertain. An attempt will now be made to characterize the growth mechanism of austenite formation responsible

for the observed effects. The two alternatives which fall under the general category of thermally activated growth are those involving (a) long range atom redistribution and (b) short range atom transport across an incoherent interface.[1]

Karlyn, Cahn, and Cohen[42] have suggested a criterion which can be used to determine if bulk diffusion ahead of an advancing interface can control the rate of growth. They show that if the observed steady state growth rate is greater than about $10^8 D$ cm/s no significant concentration gradients can be present ahead of the interface. (Here D is the diffusion coefficient in the parent matrix of the solute species under consideration.)

A rough approximation (or at least a limiting value) of the growth rate due to the mechanism under consideration may be obtained by referring to Figure 20 which shows the progress of the thermally activated transformation in the 0.6C alloy. The heating rate in this case, up to A_s, was 3°C/s but due to the endothermic reaction decreases to about 1°C/s in the range between A_s and A_f. Note that at 499°C, Figure 20(a) there is little evidence of the thermally activated mechanism. Five degrees (and 5 seconds) later, Figure 20(b), large areas characteristic of the transformation component under consideration have nucleated and grown within the martensite plates. The larger of these areas have radii of roughly 10 microns. From this observation it can be deduced that the growth rate in this 5 sec interval was at least 2 microns/sec.

Because the temperature range during which the observed growth took place was small ($\leq$ 5°C) it will be assumed to have occurred iso-

thermally at 502°C for calculation and comparison with the criterion of Karlyn, Cahn and Cohen.[42]

Hirano et al.[43] have reported that the diffusion coefficient of Ni in ferromagnetic α iron obeys the relation

$$D_{Ni}^{\alpha} = 1.4 \exp(-58{,}700/RT) \text{ cm}^2/\text{s}$$

which at T = 775°K (502°C) is 4.4×10^{-17} cm^2/s. Therefore $10^8 D_{Ni}^{\alpha} = 4.4 \times 10^{-9}$ cm/s, which is almost five orders of magnitude slower than the observed rate of 2 μ/sec. Thus long range redistribution of the Ni atoms at this heating rate is ruled out, contrary to the proposal made by Kessler and Pitsch[12] for the thermally activated transformation noted by them in Fe-32.2 Ni heated at 0.3°C per min.

On the other hand, the diffusion coefficient of carbon in martensite has been given as[44]

$$D_C^{\alpha} = 0.02 \exp(-26{,}000/RT) \text{ cm}^2/\text{s}$$

which at 502°C is 8.3×10^{-10} cm^2/s. Comparing $10^8 D_C^{\alpha}$ cm/s with the observed growth rate indicates that carbon concentration gradients ahead of the interface would be possible. However, examination of thin foils of the two higher-carbon alloys has revealed that, at the slower rates where the thermally activated transformation is observed, much of the carbon has been removed from solution by the precipitation of cementite particles in the martensite. These particles apparently redissolve only after the transformation has occurred, and then not very rapidly. For this reason it is unlikely that the actual mechanism by which the thermally activated transformation occurs is dependent

upon long range carbon redistribution between the parent and the product phases.

The transformation characteristics noted thus far, namely, (1) apparent thermal activation, (2) absence of sharp surface tilting, (3) relatively low defect density compared to the product of the martensitic-type transformation, and (4) absence of long range substitutional solute redistribution suggest that the mode of transformation in question may be classed as "massive" [45] or short range diffusion (SRD), the latter term being more descriptive of the actual transformation mechanism. [46]

The SRD transformation mechanism involves short range atom movement across a relatively high-energy interface but no change in overall composition from one side of the moving interface to the other. [1,42,45] Although most often noted in alloys of critical composition which can be cooled or heated from one single phase field in the equilibrium diagram to another at a rate rapid enough to suppress phase separation in the intervening two-phase region, there appears to be no reason why the SRD transformation could not involve metastable phases of like composition, [42,45] as in the present case.

For nearly all materials in which an SRD transformation is observed, a martensitic transformation is also possible. If the driving forces necessary for the two alternative mechanisms do not differ greatly then the temperature ranges for the two should overlap and in a continuous heating experiment it should be possible to observe a mixed transformation providing also that sufficient thermal activation is available for the SRD component. [1,45,46] Such behavior has been reported

for a number of alloys under certain conditions.[16,18,47] Massalski[45] suggests that a mixed mechanism might display nucleation that has martensitic features followed by SRD growth, a situation that would be quite possible in the present case. The extent to which martensitic nucleation-SRD growth might occur cannot be determined from the available evidence.

F. Mechanical Properties

In addition to the work regarding the effect of heating rate on the transformation characteristics, it was desired to establish the effect of heating rate on the mechanical properties of the four Fe-Ni-C alloys. Tensile specimens were tested corresponding to six separate conditions for each alloy: uncycled (conventionally annealed) austenite and austenite subjected to one cycle of $\gamma \rightarrow \alpha' \rightarrow \gamma$ transformation at nominal heating rates of 3°C/s and 1500°C/s as well as martensitic specimens formed by cooling the austenitic specimens in each condition to -196°C in liquid nitrogen just prior to testing. The mechanical properties of the austenitic and martensitic specimens will be discussed separately.

The strengthening response due to cyclic phase transformation depends upon relative changes in solid solution, carbide dispersion, dislocation substructure, and grain or subgrain size strengthening components. At least one attempt has been made to quantitatively assess these strengthening contributions,[8] however, such a quantitative treatment in the present case would require many simplifying assumptions as well as numerical evaluation of such parameters as dislocation density and carbide sizes and spacings. The fine structure of the cycled specimens exhibited complex and often inhomogeneous features, making such evaluations questionable. The discussion of the mechanical properties of austenitic and martensitic specimens in the following sections will therefore necessarily be qualitative.

1. Mechanical Properties of Austenitic Specimens

Table IV presents the results of tensile tests performed on

austenitic specimens of the four alloys under investigation. In contrast to the two lower-carbon alloys, the load-elongation curves of all austenitic specimens of the 0.3C and 0.6C alloys exhibited distinct serrations consisting of short periods of rapid elongation accompanied by sharp drops in load. That these serrations were a result of the formation of martensite during tensile testing was confirmed by noting that the gage lengths of the previously completely austenitic specimens of the 0.3C and 0.6C alloys became increasingly ferromagnetic with strain. (Unlike the ferromagnetic austenites of the 0.004C and 0.05C alloys, the austenites of the two higher-carbon alloys are paramagnetic.) The serrations identify the martensite that formed as strain-induced, requiring plastic deformation to initiate and sustain the transformation, rather than stress-induced which would require only elastic stress.[48] The consistently higher tensile strengths and uniform elongations of the 0.3C and 0.6C alloys, as compared to the other two alloys, may therefore be attributed to their enhanced ability to strain harden by the formation of strain-induced martensite.[48,49]

For those alloys in which the strain-induced transformation was noted, the onset of the serrations invariably occurred at strains greater than that corresponding to the 0.2 pct offset. In addition to this, by its very definition,[48] strain-induced martensite cannot occur without some prior plastic strain. Therefore, although the elongations and tensile strengths reported are in some cases dependent upon the formation of strain-induced martensite, the 0.2 pct offset yield stress values presented are representative of the strength of the

austenitic matrices. For this reason the discussion of the mechanical properties of the austenitic specimens will be confined to the yield strengths.

Figure 36 presents the austenitic yield strength data in graphical form to facilitate comparison. The somewhat higher yield strength of the uncycled austenite of the 0.004C alloy as compared to that for the other alloys is believed to be due to the presence of coarse, regularly shaped particles which were observed to be present throughout the as-homogenized austenite matrix. Since significant amounts of Al and Ti had been added to this alloy as oxygen getters, these particles are believed to be oxides of Al and/or Ti. Although they do slightly affect the base strength, it is not felt that these coarse particles will have a significant influence on the cycled structures.

One cycle of $\gamma \rightarrow \alpha' \rightarrow \gamma$ transformation at a heating rate of 3°C/s resulted in large increases over the strength of uncycled specimens. The yield strengths reached nearly the same levels for all four alloys. This is in spite of the fact that the martensite to austenite transformation in the three higher-carbon alloys was observed to have a thermally activated component, the proportion of which appeared to increase with carbon content at heating rates of 3°C/s. The 0.004C alloy showed no evidence for a transformation mechanism other than shear. Since the thermally activated mechanism was observed to result in a relatively lower dislocation density than the shear mechanism, it might be expected that the strengthening effect due to cycling at 3°C/s would be smaller in the three higher-carbon alloys. The fact that this is not the case emphasizes the importance of other contri-

butions to the strength of slowly cycled Fe-Ni-C austenite beside dislocation density, which is reported to be the main factor in the reverse martensitic transformation strengthening of Fe-Ni alloys.[6] Such contributions apparently arise as either direct or indirect results of the presence of carbon. Residual metastable cementite particles in the cycled austenite probably provide some degree of dispersion strengthening, but, in view of the inhomogeneous distributions of large carbides observed in the 3°C/s cycled Fe-Ni-C austenite, this effect is considered to be slight.

Austenitic yield strengths slightly above those observed for the 3°C/s cycled austenite have been reported by Hyatt and Krauss[7] for quarter-inch round specimens of the 0.05C and 0.3C alloys heated 10°C above A_f by immersion in molten salt. However, these investigators observed a comparatively smaller austenitic strengthening response in the 0.6C alloy and attributed this to the extensive recrystallization processes in the austenite due to the anomolously high A_f (740°C) determined for that alloy. The results of the present investigation show the A_f for this alloy is only slightly above that for the 0.3C alloy and, although much of the austenite formation at 3°C/s occurs by the thermally activated mechanism, the strengthening response is not affected.

An increase in heating rate from 3°C/s to 1500°C/s resulted in considerable improvements in the yield strengths of cycled austenites of the higher carbon alloys but had essentially no effect on the 0.004C alloy. Notice that the increment of austenitic strengthening due to rapid heating increases with alloy carbon content. It is likely that

the enhancement of the strengthening response due to rapid compared with slow heating is brought on by either or both of two separate phenomena. First, the thermally activated component of transformation was demonstrated to be suppressed by high heating rates. Suppression of this mode of transformation in a given alloy should result in the higher dislocation densities characteristic of the shear transformation and greater strength. Another effect of increasing heating rate is to alter the carbide distribution in the parent martensite as well as in the cycled austenite. As was demonstrated in the Electron Microscopy section, increasing the heating rate from 3°C/s to 1500°C/s resulted in somewhat smaller carbides, more uniformly distributed in the parent martensite of the 0.3C alloy. Although the same distribution of particles observed in the martensite heated just below A_s was not seen in cycled austenite specimens of the 0.3C alloy given the standard reversal treatment at 1500°C/s (Figure 28), it is quite possible that a uniform distribution of cementite particles in the parent martensite could aid in strengthening the product by acting as dislocation multiplication and pinning sites, thus enhancing the effect of the shear-type transformation to austenite.

In an attempt to assess the degree to which tempering processes in the parent martensite influence the austenite strengthening response due to cyclic transformation, tensile specimens of the 0.3C alloy which had been pretempered by heating to 400°C at 3°C/s before austenitizing at 1500°C/s were tested in the cycled austenite condition. The average yield strength of such pretempered specimens (89 ksi) was slightly below that of the standard 1500°C/s cycled specimens (98 ksi) but well

above that for the 3°C/s cycled specimens (72 ksi). The only obvious difference between the fine structures of the pretempered and conventional rapidly reversed specimens (Figures 30 and 28, respectively) are the occasional rows of well-defined carbides observed in the former. The above results indicate that changes in carbide distribution within the range of distributions attainable at heating rates between 3°C/s and 1500°C/s play a relatively minor role in determining the cyclic transformation strengthening response of the 0.3C alloy. A more important factor in this alloy is probably suppression of the thermally activated component by high-rate heating, resulting in a more fragmented substructure and a higher dislocation density.

The benefits of rapid heating during the $\alpha' \rightarrow \gamma$ transformation were most marked in the 0.6C alloy where a 30 ksi increment of austenite strengthening was realized by increasing the heating rate from 3°C/s to 1500°C/s. The reason for this is evident in the substructure of the rapidly heated austenite, Figure 32, which, in comparison with slowly austenitized structure in Figure 31, was seen to contain a more uniform fine structure consisting of a high dislocation density in addition to many large and small carbide particles.

It is interesting to note that, except for the 0.3C alloy in which a large amount of strain-induced martensite formed during tensile testing, the yield strength levels attained by cycling were significantly higher than the uncycled tensile strengths in a given alloy. This indicates that the operative strengthening mechanisms in the cycled austenitic structures are much more effective than simple strain-hardening.

2. Mechanical Properties of Martensitic Specimens

Table V presents the complete results of tensile tests performed on the martensitic specimens and Figure 37 shows the yield strengths in relation to one another. No data was obtained for the uncycled martensite of the 0.6C alloy because the specimens invariably broke before the 0.2 pct offset yield strain was reached. The mechanical properties established by Hyatt and Krauss[7] for the uncycled martensite of the 0.6C alloy are given for comparison.

In contrast to the austenitic specimens, the strengthening increments in martensitic specimens due to cycling were modest in all alloys in agreement with previous investigations in Fe-Ni[5] and Fe-Ni-C alloys.[7,8] Indeed, the yield strengths of cycled specimens of the 0.6C alloy fall in the same range as those of the 0.3C alloy and are well below the value determined by Hyatt and Krauss[7] for uncycled martensite in the 0.6C alloy. A possible reason for this will be discussed below. It should also be noted that the amount of martensite present in the cycled specimens of a given alloy was consistently smaller than in the uncycled specimens. This effect tends to lower the apparent cyclic transformation strengthening response of martensitic specimens.

Significant additional increases in martensitic strengths of the 0.05 and 0.3C alloys were obtained by heating at the faster rate. That the 0.004C alloy showed essentially no change in strength on increasing the heating rate is not surprising in view of the fact that the same effect was observed on cycling the austenitic specimens. The 0.6C alloy, which had registered the greatest austenitic strength increases

upon increasing the heating rate, showed no significant response to increased heating rates. These unexpected results are undoubtedly due to the depletion of carbon from interstitial solid solution. As shown in Figures 31 and 32, coarse residual cementite particles were observed in the cycled austenitic matrix of this alloy after heating at both 3°C/s and 1500°C/s. These coarse particles would provide only weak dispersion strengthening of the cycled structures. However, the precipitation of these particles can come about only at the expense of interstitial carbon. Carbon in solution has a relatively minor effect upon the strength of austenite[50] but an extremely large effect on the strength of martensite.[30,51] Therefore, while the austenite may be strengthened to some degree by cyclic heat treatment, it is possible for the corresponding martensitic structure to be weakened.[52]

By far the best results in terms of balance of martensitic properties were realized in the 0.3C alloy. In this alloy yield strengths of 24 ksi over the uncycled martensite were obtained by rapid austenitization and this strength increase was accompanied by a significant enhancement of uniform elongation. While roughly the same increment of strengthening was seen for the 0.05C alloy, the strength increases occurred at the expense of uniform elongation.

CONCLUSIONS

1. The A_s temperatures of the 0.05, 0.3, and 0.6C alloys show a slight tendency to decrease with increasing heating rate between 3°C/s and 28,000°C/s. The A_f data of the 0.004C alloy was insufficient to indicate a trend.
2. The A_f temperatures of the three higher-carbon alloys display a complex relationship to heating rate, initially increasing by as much as 50°C with increasing heating rate and eventually reaching a maximum and decreasing with further increases in heating rate. The 0.004C alloy showed no change in A_f over the entire range of heating rates used.
3. The $\alpha' \rightarrow \gamma$ transformation was seen to occur by two separate, often competing mechanisms in the three higher-carbon alloys. One mechanism is accompanied by the tilt-type surface relief characteristic of a martensitic-type transformation. Austenite areas formed by this mechanism are acicular and contain the high dislocation densities characteristic of a martensitic transformation.
4. The other $\alpha' \rightarrow \gamma$ transformation mechanism is thermally activated and apparently involves short range diffusion across an incoherent interface. Only the rounded relief features which can be attributed to a volume change accompany this mechanism and the austenite formed in this manner has dislocation densities relatively lower than the γ formed by the martensitic mechanism but still significantly higher than in annealed γ.

5. The thermally activated transformation can be suppressed by rapid heating, which accounts for the large initial increase of A_f with heating rate. The general features of the A_s and A_f vs. heating rate curves can be explained qualitatively on the basis of a mixed transformation mechanism, eventually becoming predominantly martensitic in nature as the heating rate is increased.

6. Tempering processes in the parent martensite, in particular cementite formation, occur very rapidly during the heating cycle and, along with the transformation mechanism, make the substructure developed in the cycled austenite quite dependent upon heating rate.

7. Austenitic specimens of all four alloys cycled at 3°C/s were greatly strengthened compared to uncycled specimens and in the three higher-carbon alloys, cycling at 1500°C/s resulted in significant additional strengthening, reflecting the changes in transformation mechanism. For example, the 0.3C alloy yield strengths were 21, 72, and 98 ksi for uncycled, 3°C/s cycled and 1500°C/s cycled austenites, respectively. The 0.004C alloy showed no response to increased heating rate in accord with the single transformation mechanism operating over the entire range of heating rates.

8. The strengths of martensitic specimens responded more modestly to cycling. Increases of from 10 to 16 ksi were observed after $\alpha' \rightarrow \gamma \rightarrow \alpha'$ transformation in the 0.004, 0.05, and 0.3C alloys when the heating rate was 3°C/s, even though the amount of retained austenite increased after cycling. However, only in the

0.05 and 0.3C alloys did increasing the heating rate enhance the strengthening response of martensitic specimens.

9. Cycling at both 3°C/s and 1500°C/s appeared to be deleterious to martensitic strengths of the 0.6C alloy, due in large part to excessive tempering during the heating cycle and the large attendant loss of solid solution strengthening which substructural strengthening effects could not fully compensate.

APPENDIX

Elimination of Non-Thermal EMF by Use of a Thermotrio

The thermotrio circuit can be represented schematically as in Figure 38(a) where R_{S1} and R_{S2} represent the small resistance of the specimen between the two outer (chromel) leads and the center (alumel) lead. R_1 represents the total resistance of the 10 Ω potentiometer which is divided into R_{1a} and R_{1b}, the ratio of which depends upon the position of the wiper arm. The circuit shown constitutes a voltage divider network and it can be seen from inspection that in the absence of a temperature difference between the specimen and the cold junction, the cold junction voltage, V_{cj}, will be zero when R_1 is adjusted so that $R_{1a}/R_{1b} = R_{S1}/R_{S2}$.

As the temperature of the specimen increases relative to the cold junction, the ratio R_{S1}/R_{S2} should not change and the cold junction voltage, V_{cj}, should then be due only to thermal emf. This situation is shown in the simplified schematic in Figure 38(b) where V_{T1} and V_{T2} represent the thermal emf's of the two thermocouples with a common alumel junction and whose chromel leads are joined across R_1. Again, a voltage divider network is established and it can be seen that the voltage measured, V_{cj}, will be between V_{T1} and V_{T2}, depending upon the ratio R_{1a}/R_{1b} which had been previously set in eliminating the non-thermal component. Since the two chromel leads are only approximately 0.040 in. apart, the temperatures at the chromel junctions should not differ significantly and hence V_{T1} and V_{T2} should be essentially the same, making V_{cj} an accurate indication of the temperature.

TABLE I - CHEMICAL ANALYSES OF ALLOYS (WT PCT)

ALLOY	C	Ni	Mn	P	S	Si	Cr	Mo	Al	N	O	Ti
0.004C	0.004	32.2	-	-	-	-	-	-	0.072	-	-	0.1
0.05C	0.05	30	0.005	0.002	0.003	0.01	0.001	0.001	0.015	0.001	0.0017	-
0.3C	0.29	24.9	0.001	0.005	0.003	0.01	0.003	0.001	0.012	0.001	0.0011	-
0.6C	0.60	21.9	0.002	0.004	0.003	0.01	0.002	0.001	0.015	0.001	0.0006	-

TABLE II

AUSTENITE GRAIN SIZES AFTER HOMOGENIZATION

AT 1100°C FOR 2 HOURS

ALLOY	ASTM GRAIN SIZE
0.004C	1
0.05C	3-4
0.3C	4-5
0.6C	3-4

TABLE III

COMPARISON OF A_f AND AVERAGE REVERSAL TEMPERATURES

	3°C/s		1500°C/s	
Alloy	A_f, °C	Ave. Reversal Temperature, °C	A_f, °C	Ave. Reversal Temperature, °C
0.004C	368	405	368	420
0.05C	425	465	433	494
0.3C	493	520	536	580
0.6C	515	545	553	591

TABLE IV

SUMMARY OF TENSILE DATA FOR SPECIMENS

IN THE AUSTENITIC CONDITION*

	CONDITION	Y.S., KSI	T.S., KSI	%E(uniform)
0.004C	Uncycled	37.0	68.4	23
	Cycled			
	3°C/s	74.7	86.1	5.3
	1500°C/s	75.9	87.9	4.7
0.05C	Uncycled	25.5	69.0	33
	Cycled			
	3°C/s	72	88	8.1
	1500°C/s	93	103	2.5
0.3C	Uncycled	21.1	112	71
	Cycled			
	3°C/s	72	176	35
	1500°C/s	98	179	43
0.6C	Uncycled	28	93	38
	Cycled			
	3°C/s	76	150	17
	1500°C/s	106	144	19

*Averages of at least three tests in each condition.

TABLE V

SUMMARY OF TENSILE DATA FOR SPECIMENS

IN THE MARTENSITIC CONDITION

	-CONDITION	Y.S.,KSI*	T.S.,KSI*	Uniform %E*	% MARTENSITE
0.004C	Uncycled	67.1	99.5	5.4	77.3
	Cycled				
	3°C/s	82.7	117	4.1	72.2
	1500°C/s	80.8	113	3.8	73.2
0.05C	Uncycled	95	141	7.7	91.4
	Cycled				
	3°C/s	105	142	2.3	88.9
	1500°C/s	120	167	4.1	88.3
0.3C	Uncycled	143	-+	1.5	89.3
	Cycled				
	3°C/s	159	242	10	83.2
	1500°C/s	167	258	9	84.9
0.6C	Uncycled	183-208**	245-278**	3**	84.6
	Cycled				
	3°C/s	169	-+	1.3	77.9
	1500°C/s	165	233	1.9	74.2

* Averages of at least four tests in each condition.

+ Specimens tended to break prematurely.

** Data reported by Hyatt and Krauss.[7]

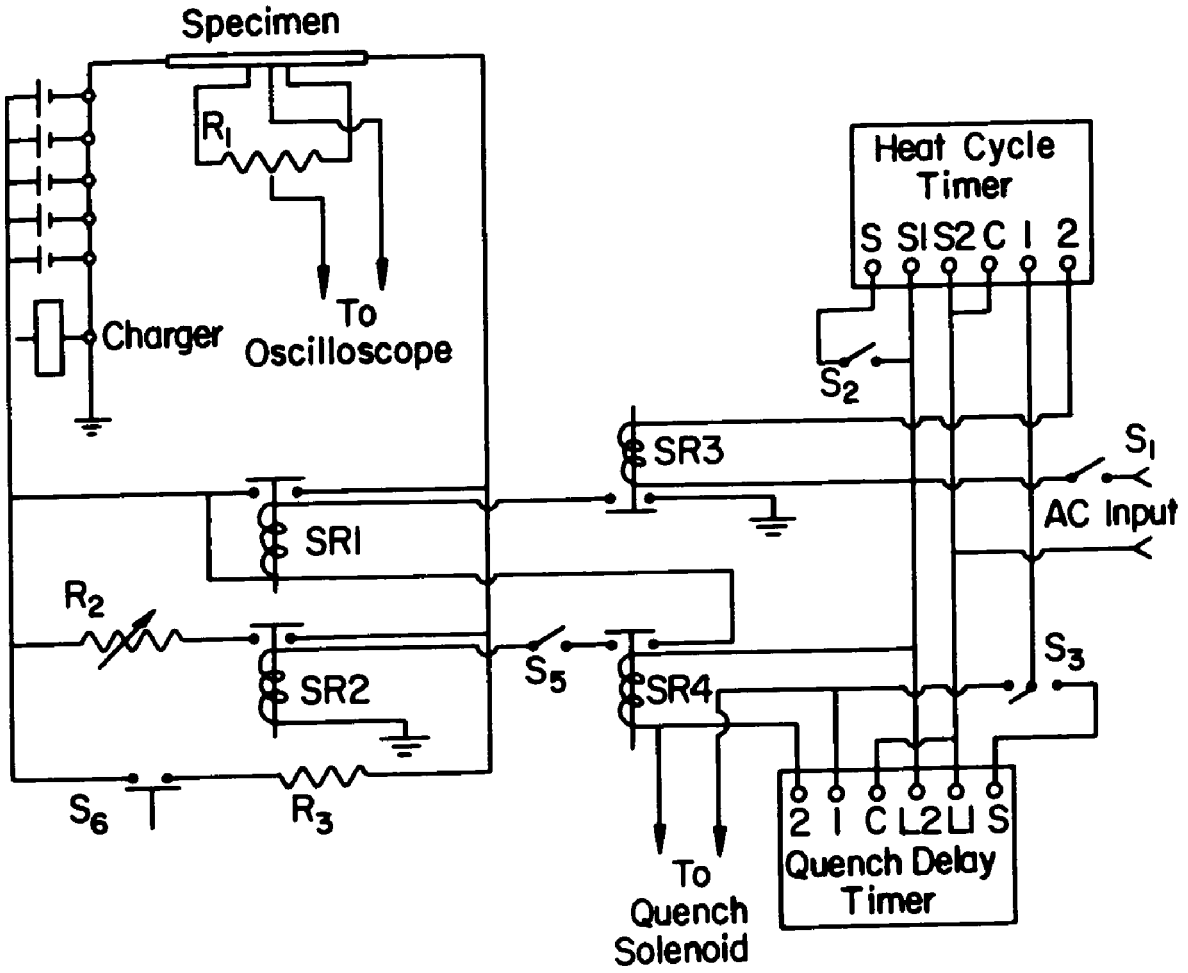

Figure 1 - Schematic diagram of direct resistance heating apparatus.

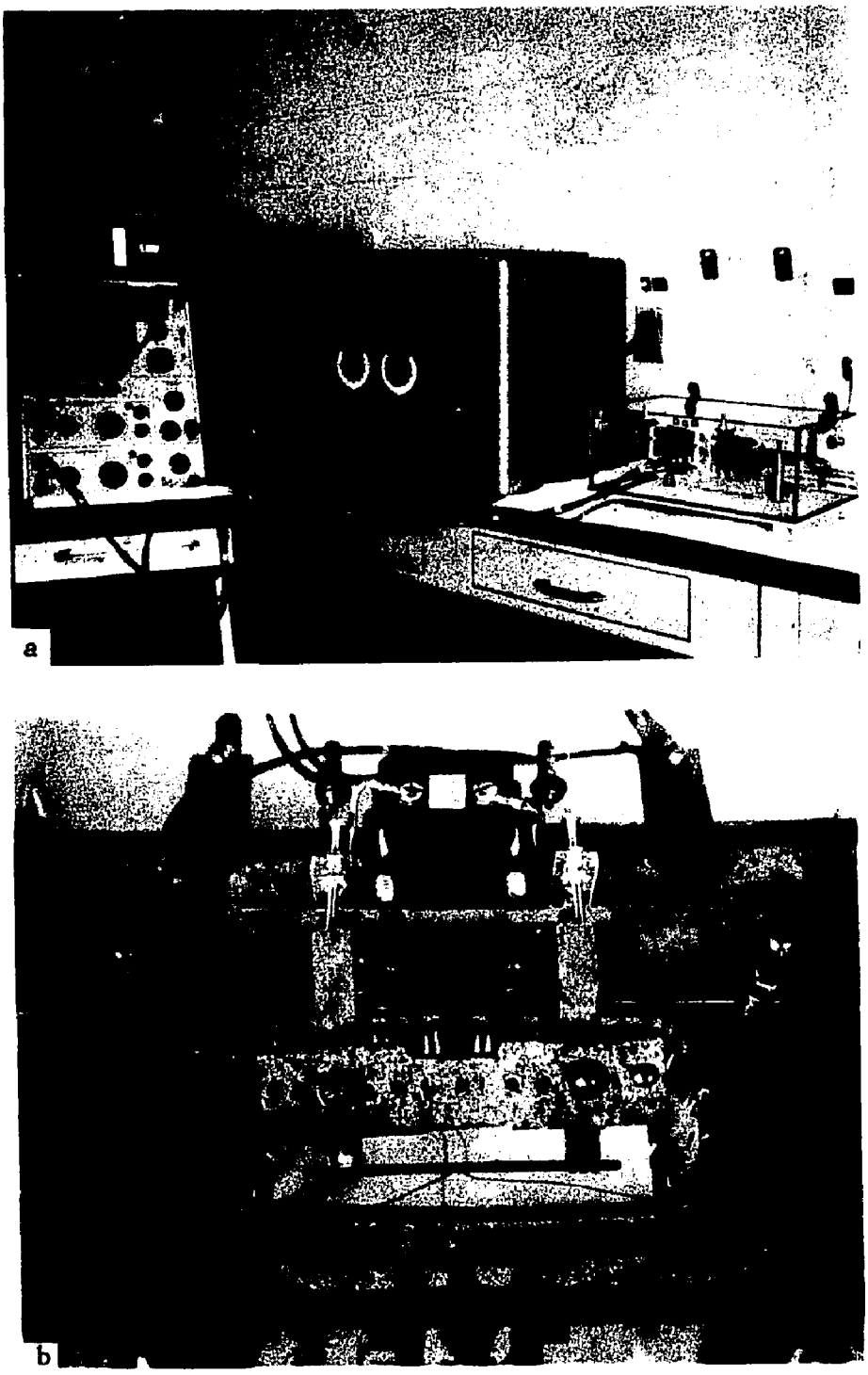

Figure 2 - Photographs of direct resistance heating unit - a) console and specimen holder with oscilloscope attached, b) quenching assembly.

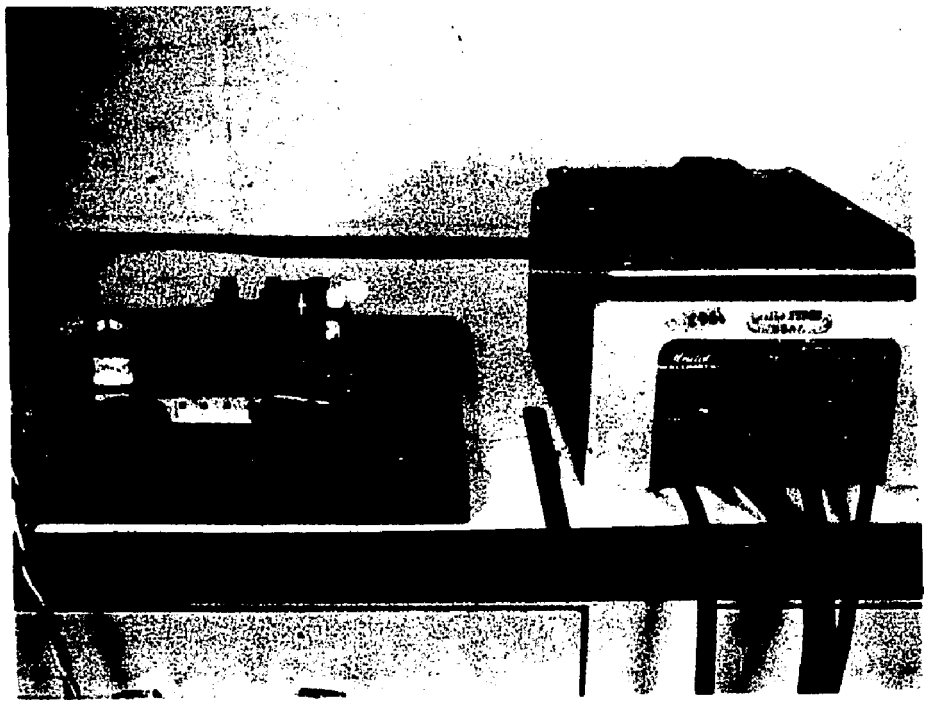

Figure 3 - Photograph of spot welder used to weld thermo-trio to specimens.

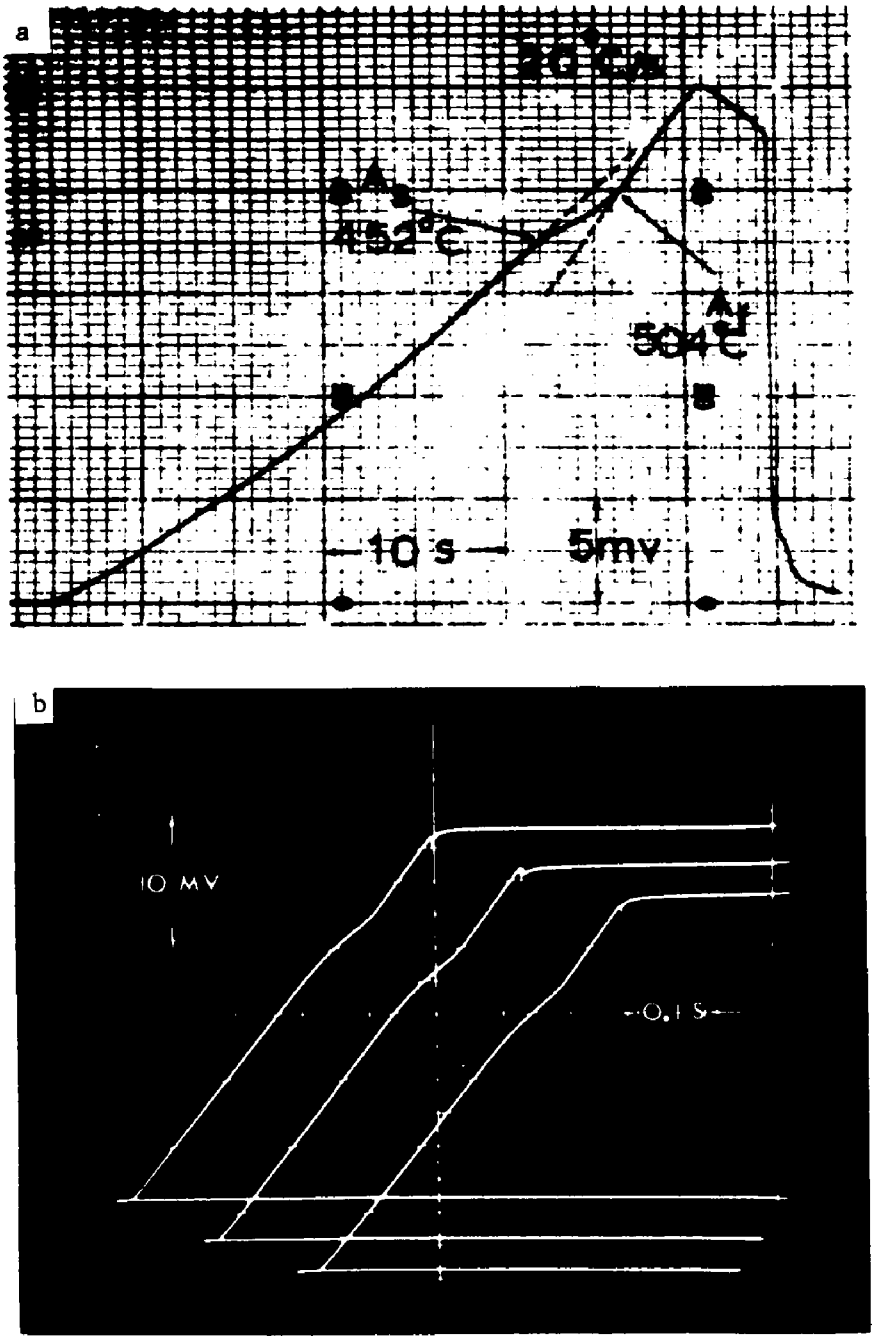

Figure 4 - Examples of T-t curves obtained on heating martensitic specimens of the 0.3C alloy - a) recorder trace (20°C/s) showing method of A_s and A_f determination, b) oscilloscope traces from three different specimens heated 1500°C/s illustrating reproducibility.

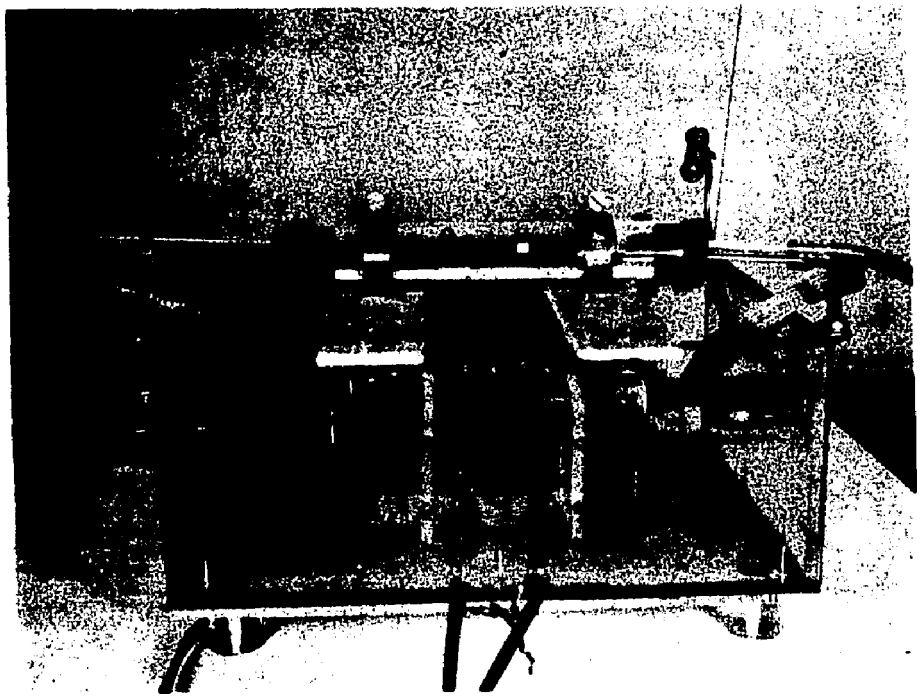

Figure 5 - Photograph of assembly for heating surface relief specimens.

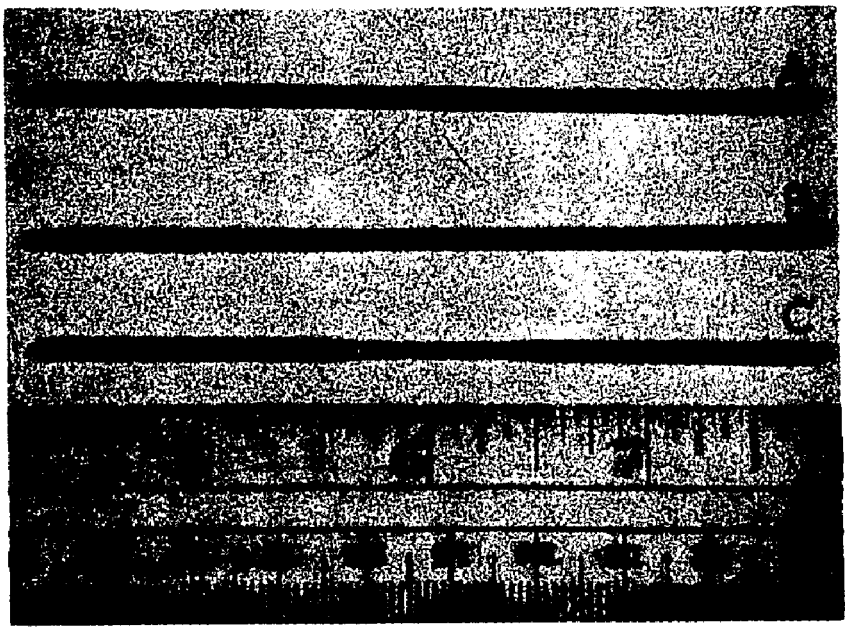

Figure 6 - Preparation of tensile specimens from 0.095 in. diameter heated rods. As-heated specimen with thermotrio, specimen lacquered at ends and finished tensile specimen shown at A, B, and C, respectively.

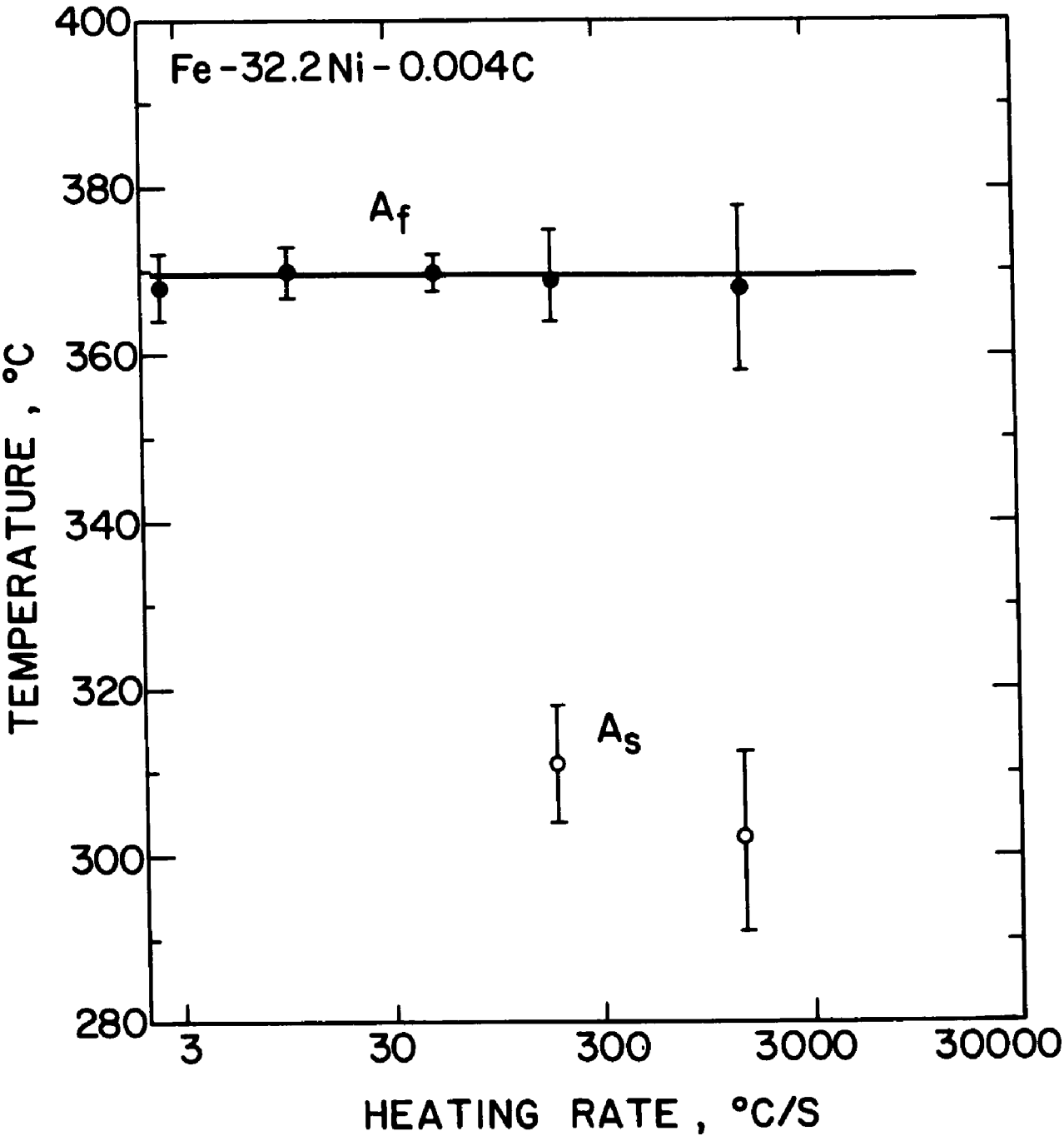

Figure 7 - A_s and A_f versus heating rate for the 0.004C alloy. Standard deviation is indicated.

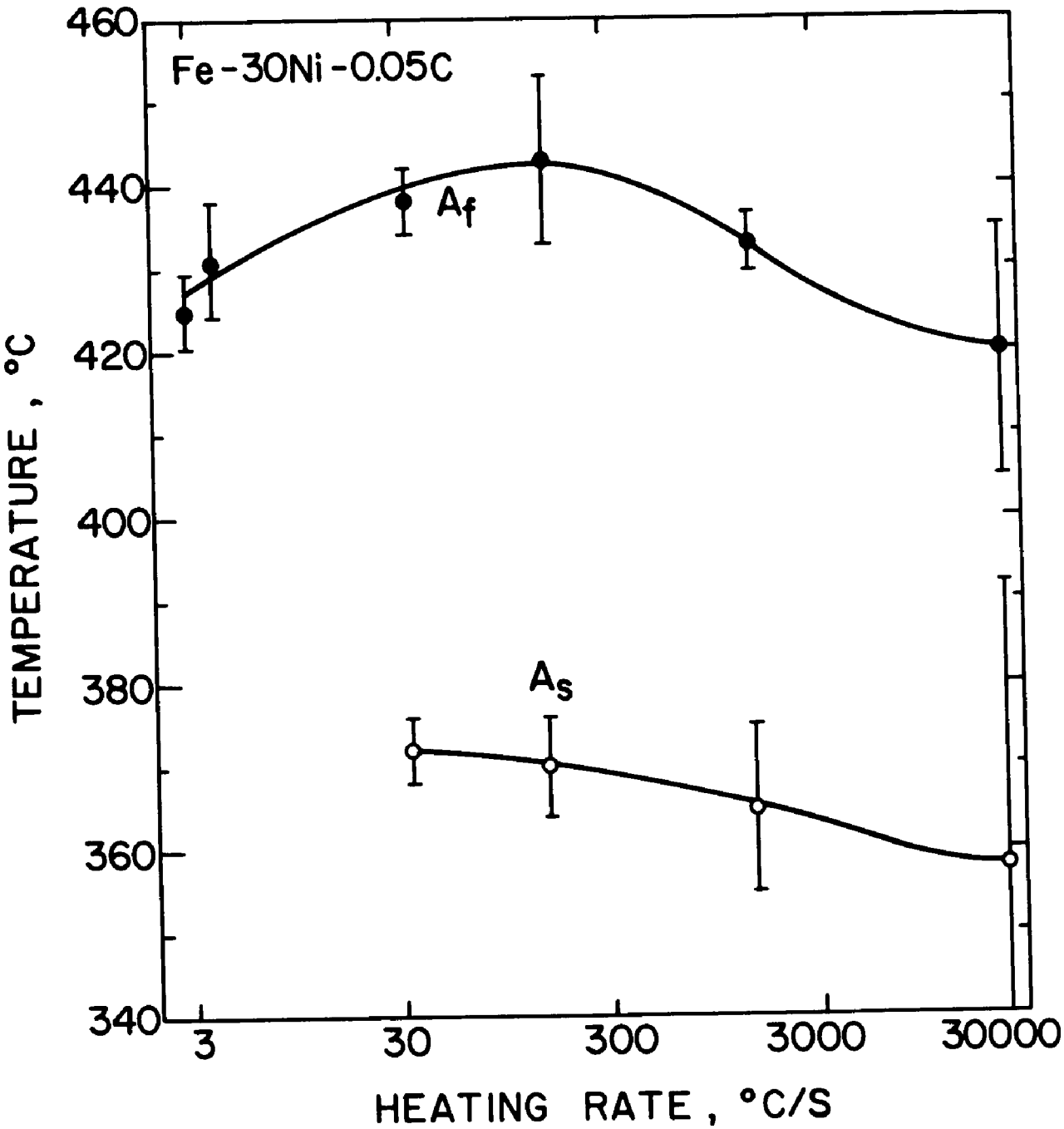

Figure 8 - A_s and A_f versus heating rate for the 0.05C alloy. Standard deviation is indicated.

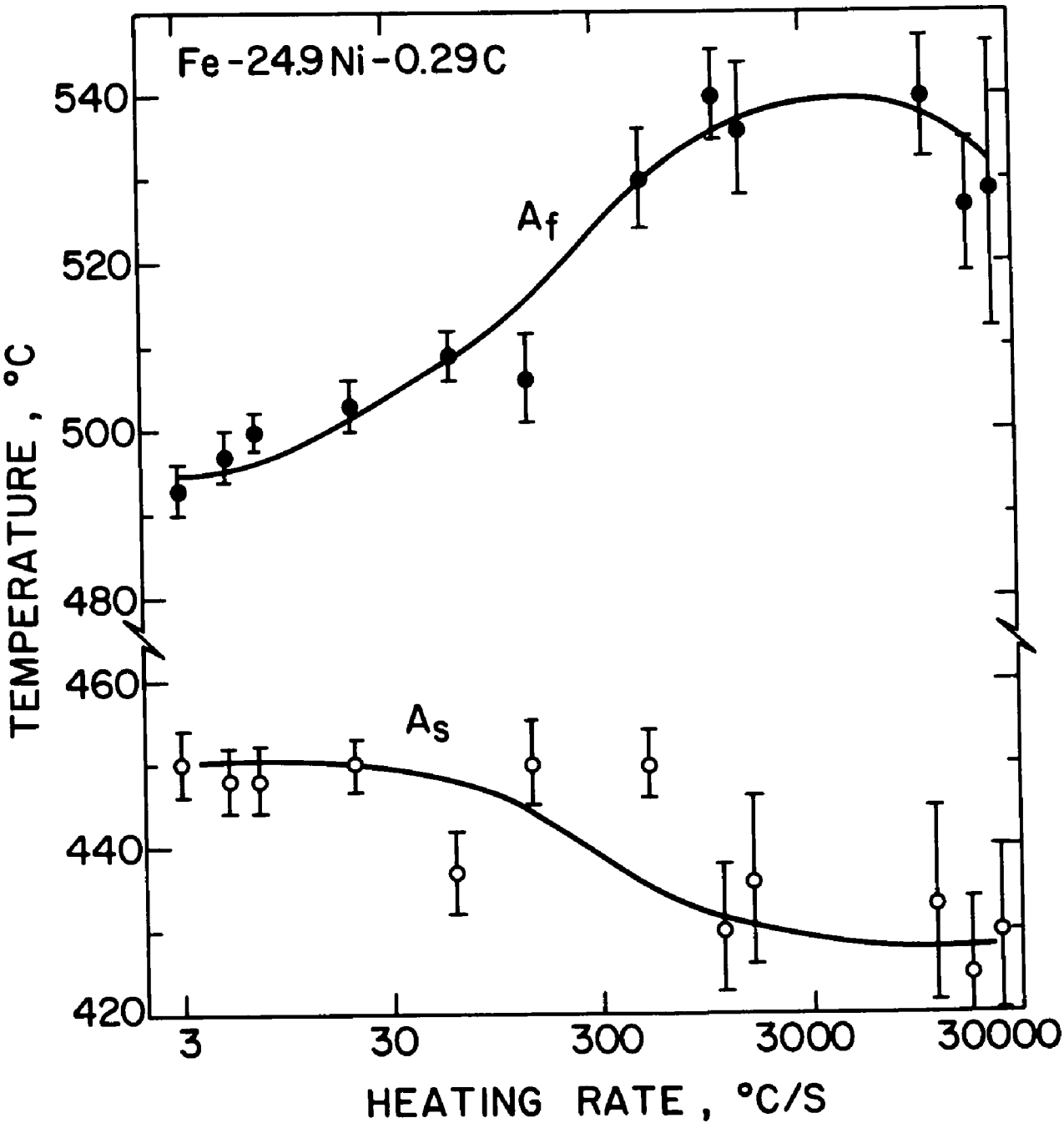

Figure 9 - A_s and A_f versus heating rate for the 0.3C alloy. Standard deviation is indicated.

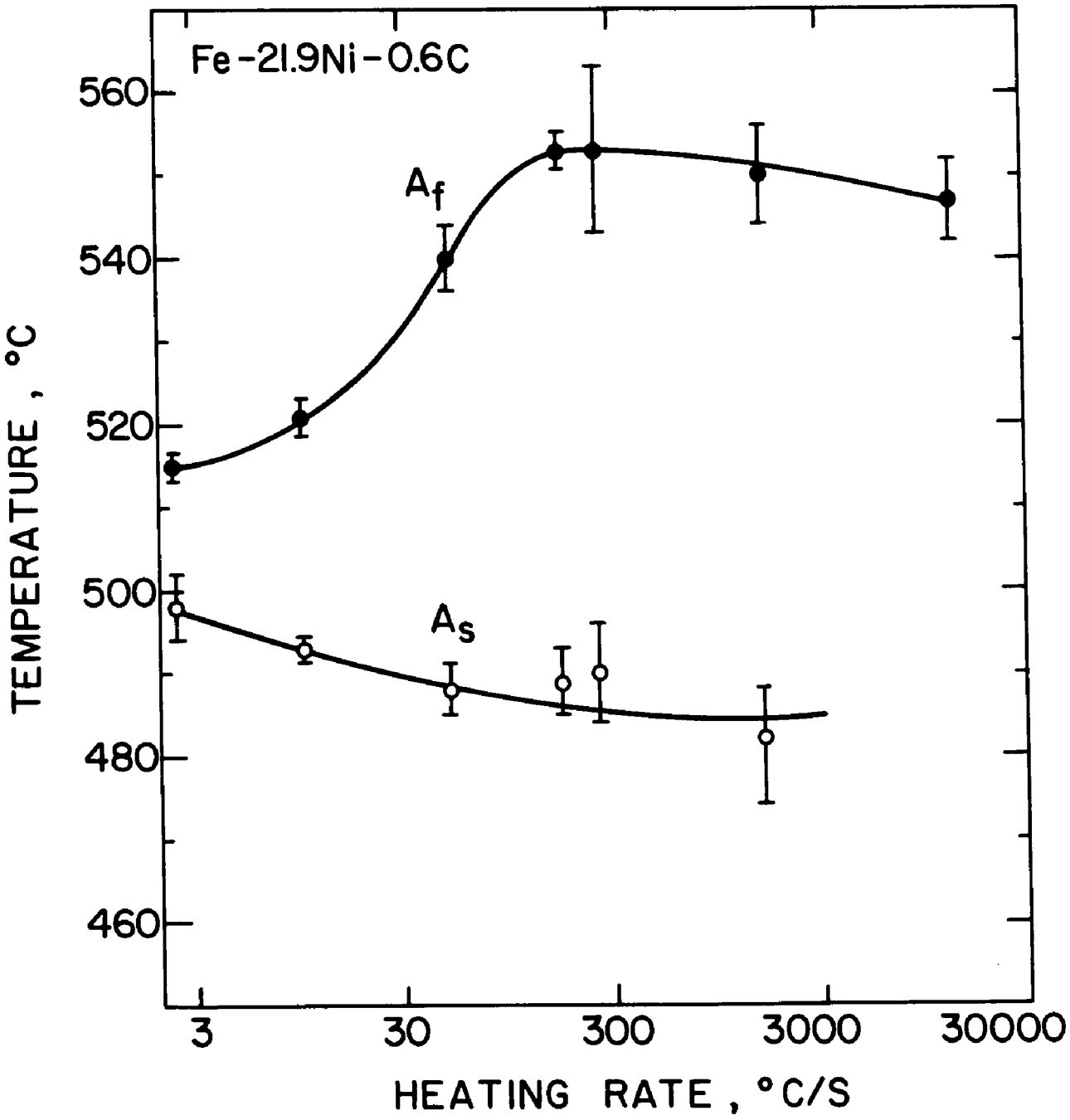

Figure 10 - A_s and A_f versus heating rate for the 0.6C alloy. Standard deviation is indicated.

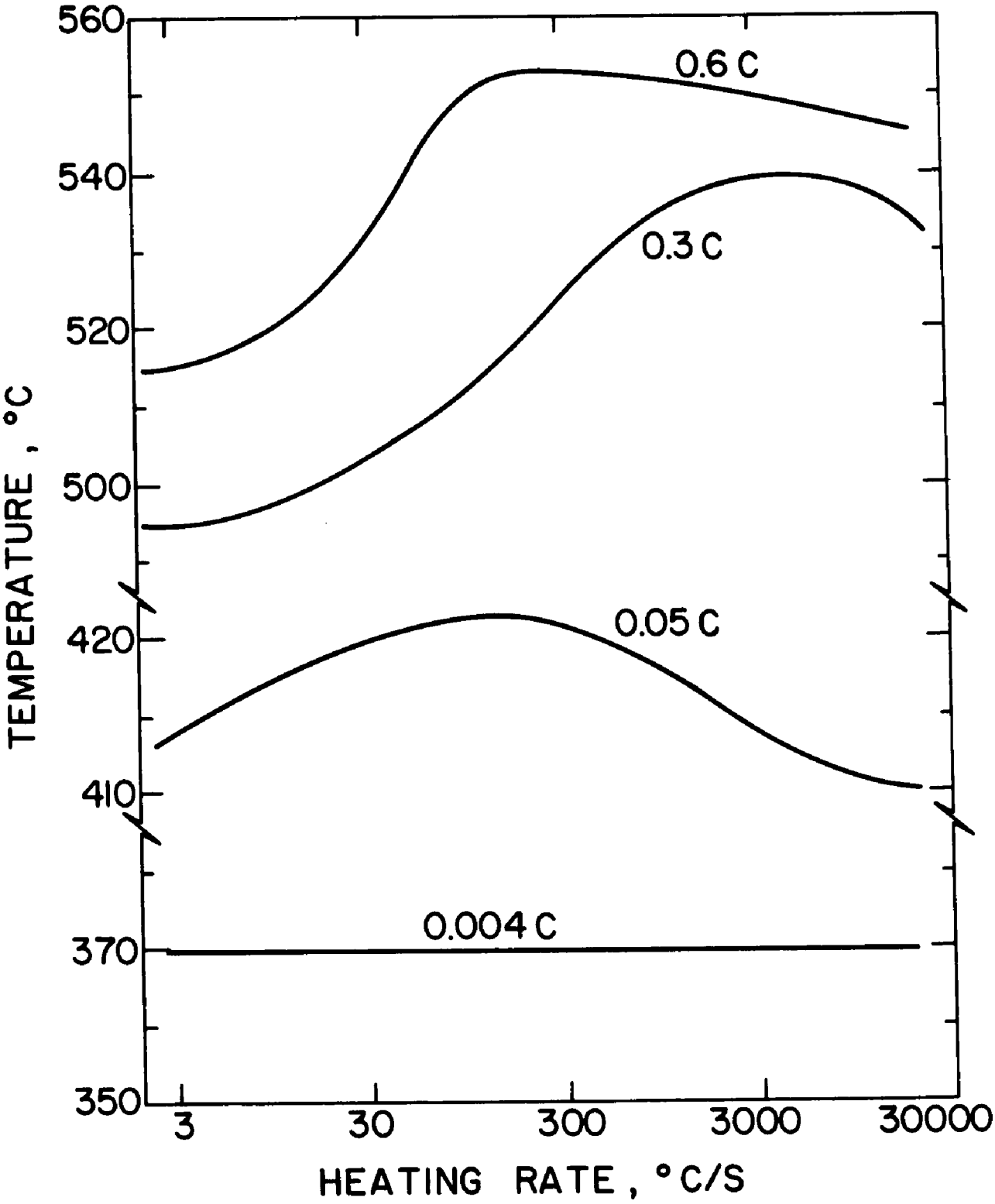

Figure 11 - A_f versus heating rate for the four Fe-Ni-C alloys. Note broken temperature scale.

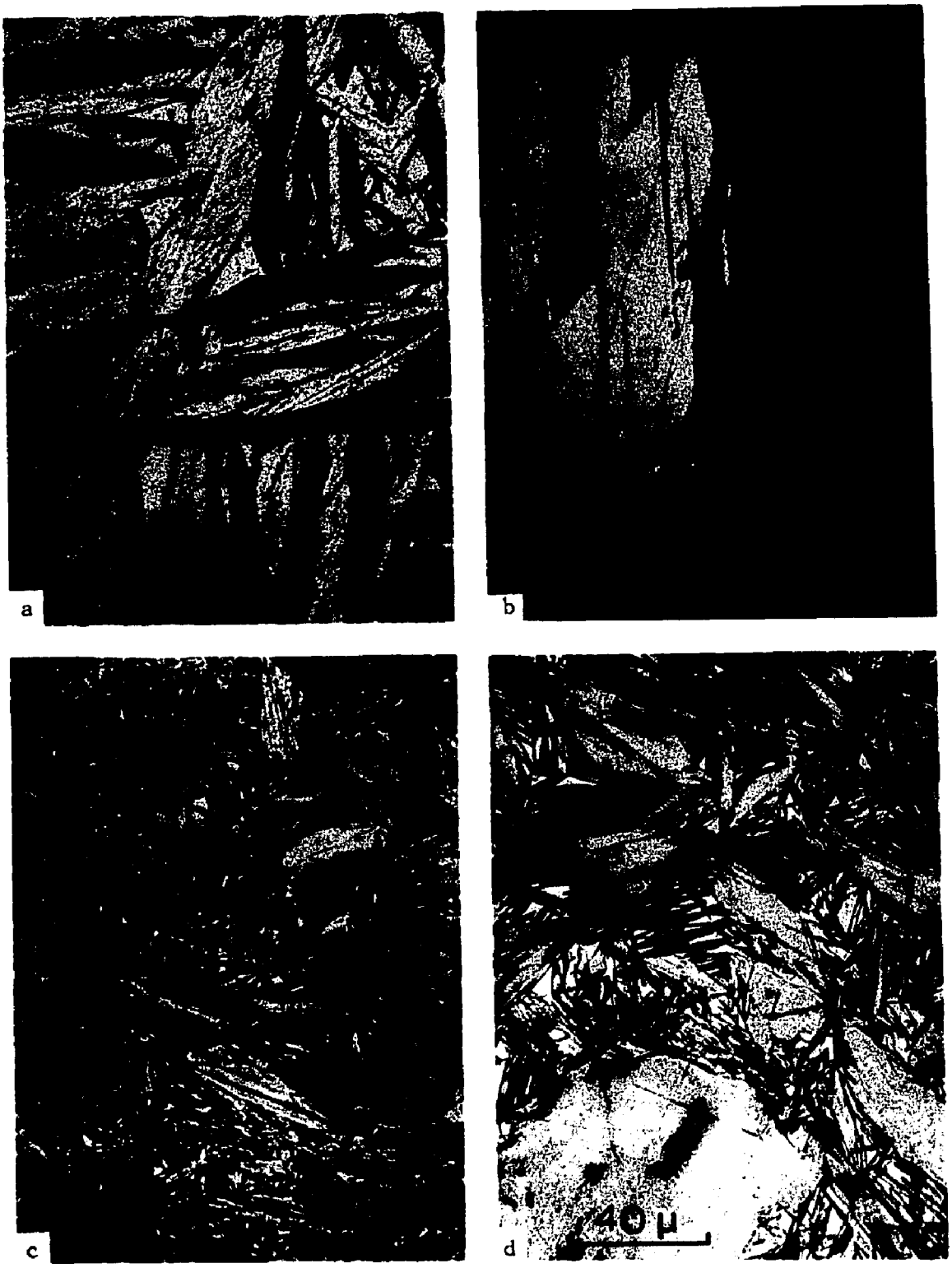

Figure 12 - Martensitic structures obtained by cooling the Fe-Ni-C alloys to -196°C - a) 0.004C alloy, b) 0.05C alloy, c) 0.3C alloy, d) 0.6C alloy. Light photomicrographs. 532X.

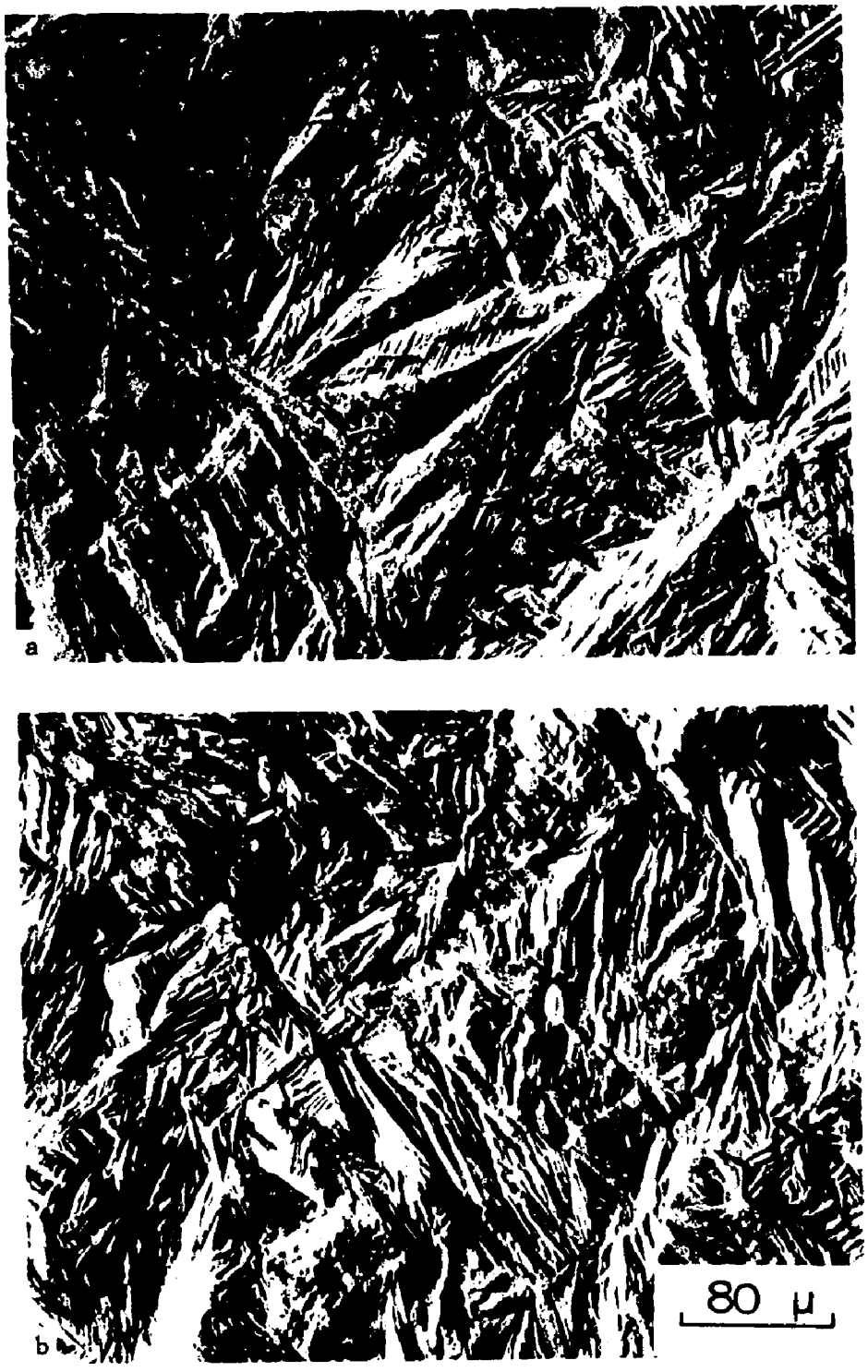

Figure 13 - Surface relief on prepolished surfaces of the 0.05C alloy completely austenitized at - a) 3°C/s and b) 3000°C/s. Light photomicrographs. 256X.

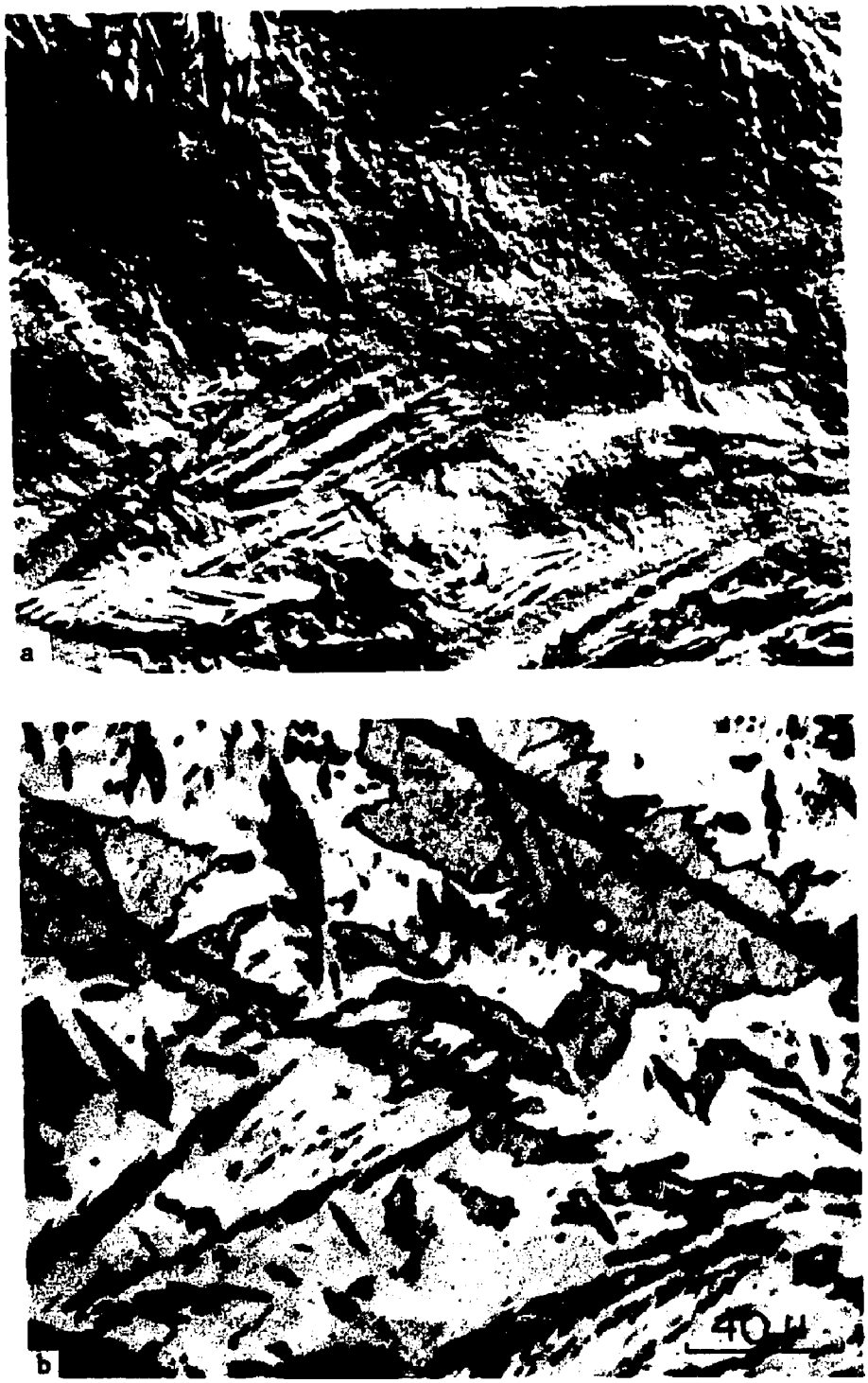

Figure 14 - Surface relief and corresponding structure of the 0.05C alloy partially austenitized at 3°C/s - a) surface relief, b) etched structure. Light photomicrographs. 512X.

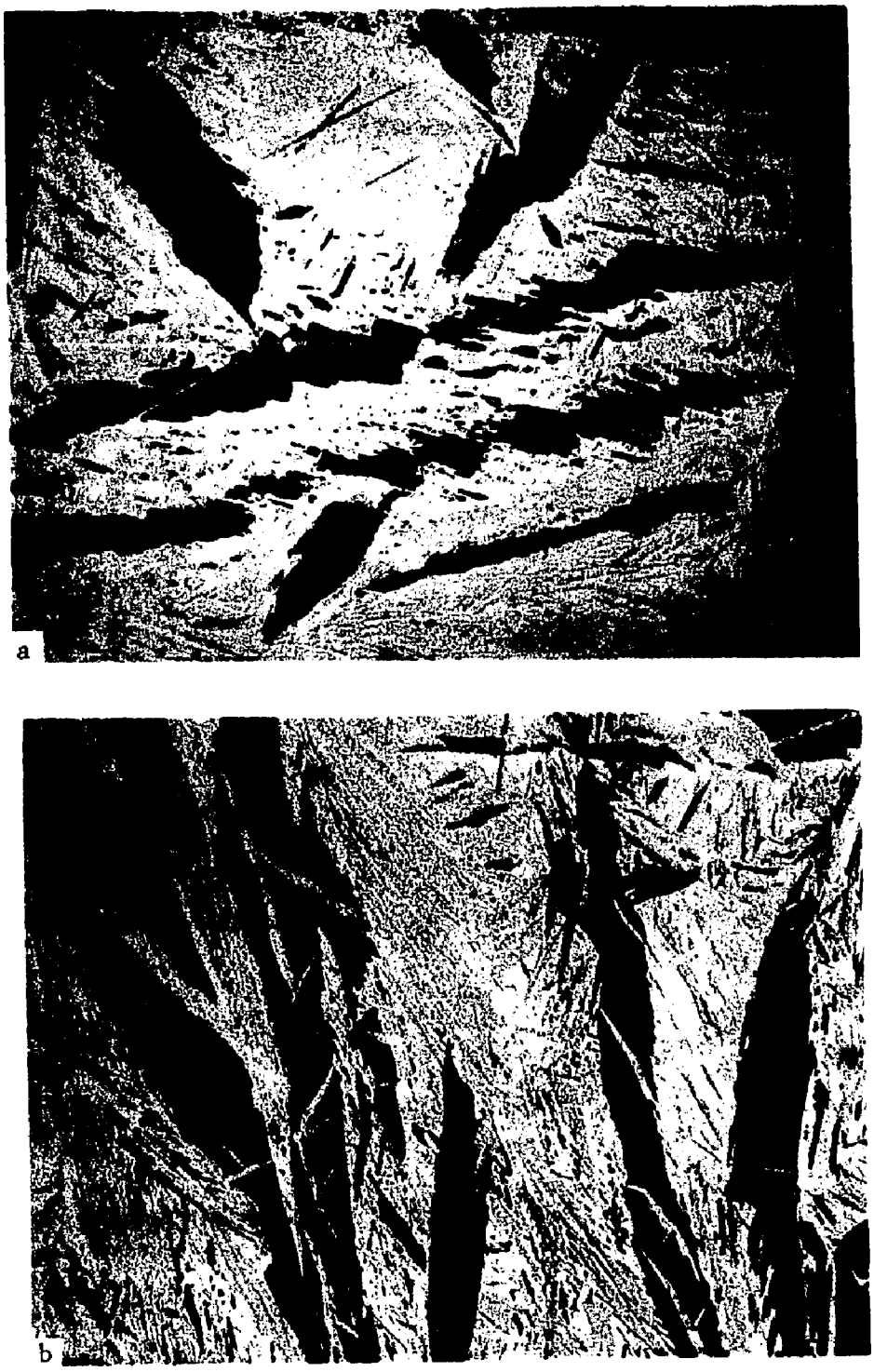

Figure 15 - Microstructures of the 0.05C alloy partially austenitized at - a) 3°C/s, and b) 1500°C/s followed by an immediate water quench. Light photomicrographs. 532X.

Figure 16 - Surface relief and corresponding structure of the 0.05C alloy partially austenitized at 3000°C/s - a) surface relief, and b) etched structure. Light photomicrographs. 512X.

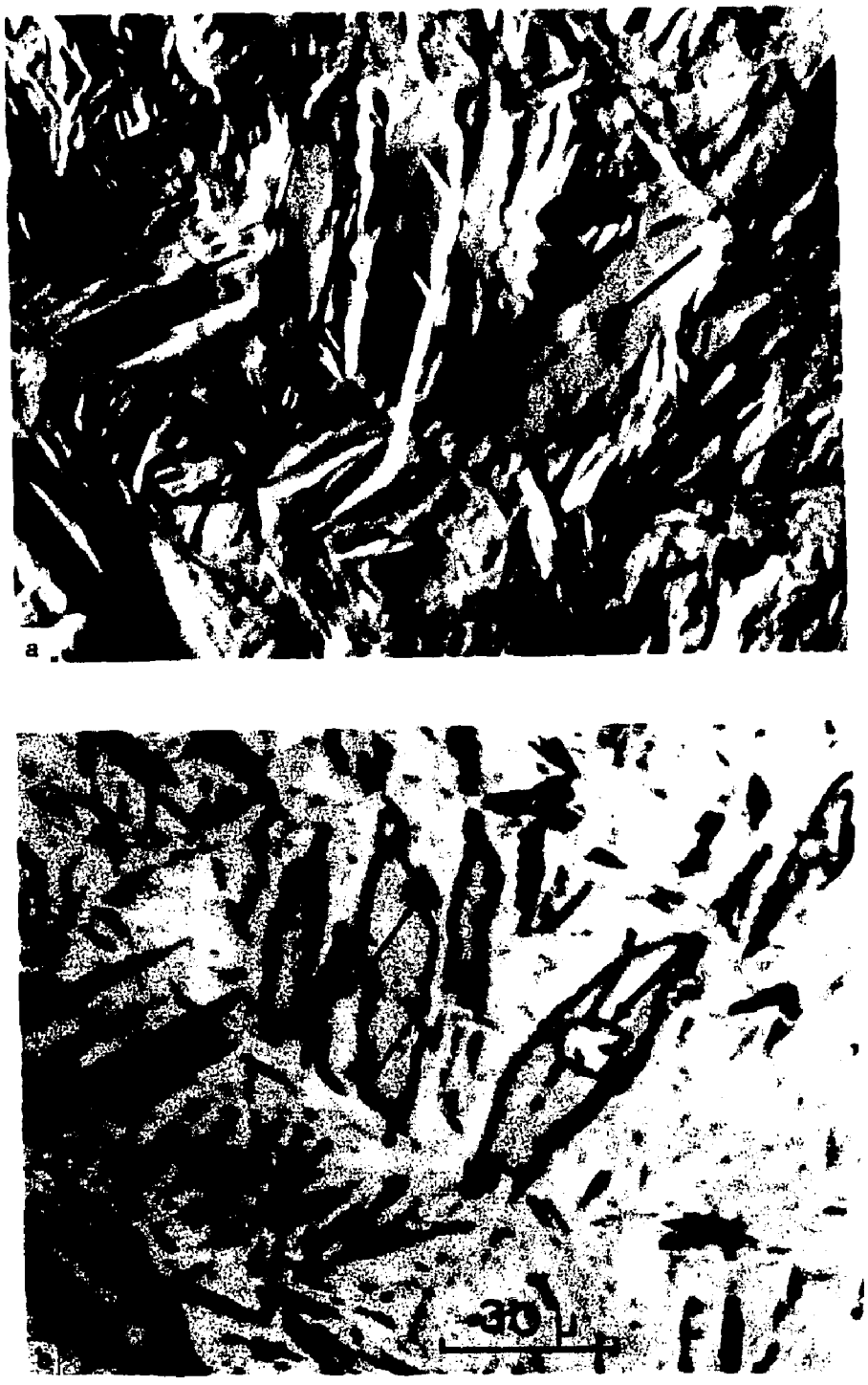

Figure 17 - Surface relief and corresponding structure of the 0.3C alloy partially austenitized at 3°C/s - a) surface relief, and b) etched structure. Light photomicrographs. 750X.

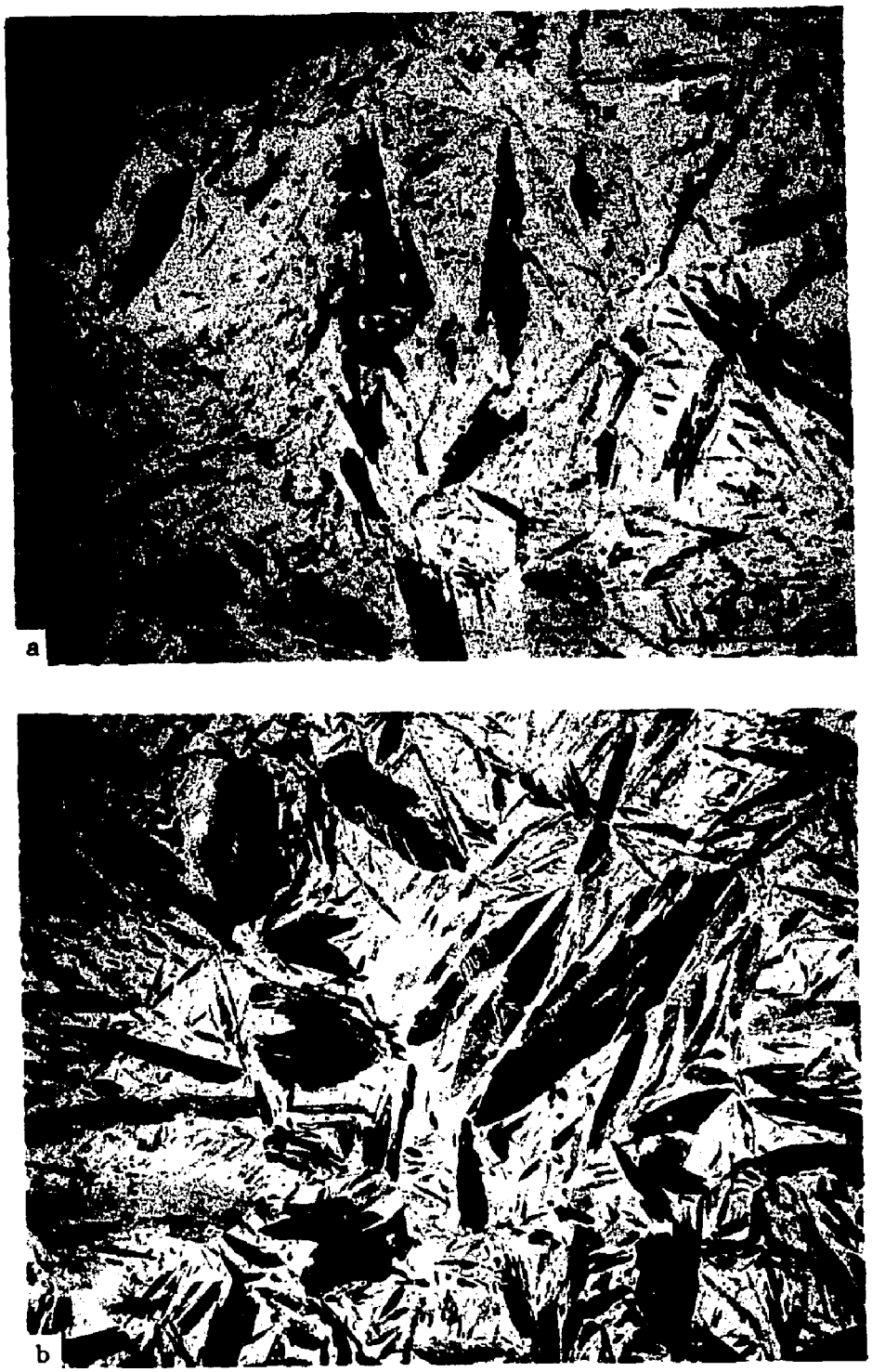

Figure 18 - Microstructures of the 0.3C alloy partially austenitized at - a) 3°C/s and b) 1500°C/s followed by a direct water quench. Light photomicrographs. 532X.

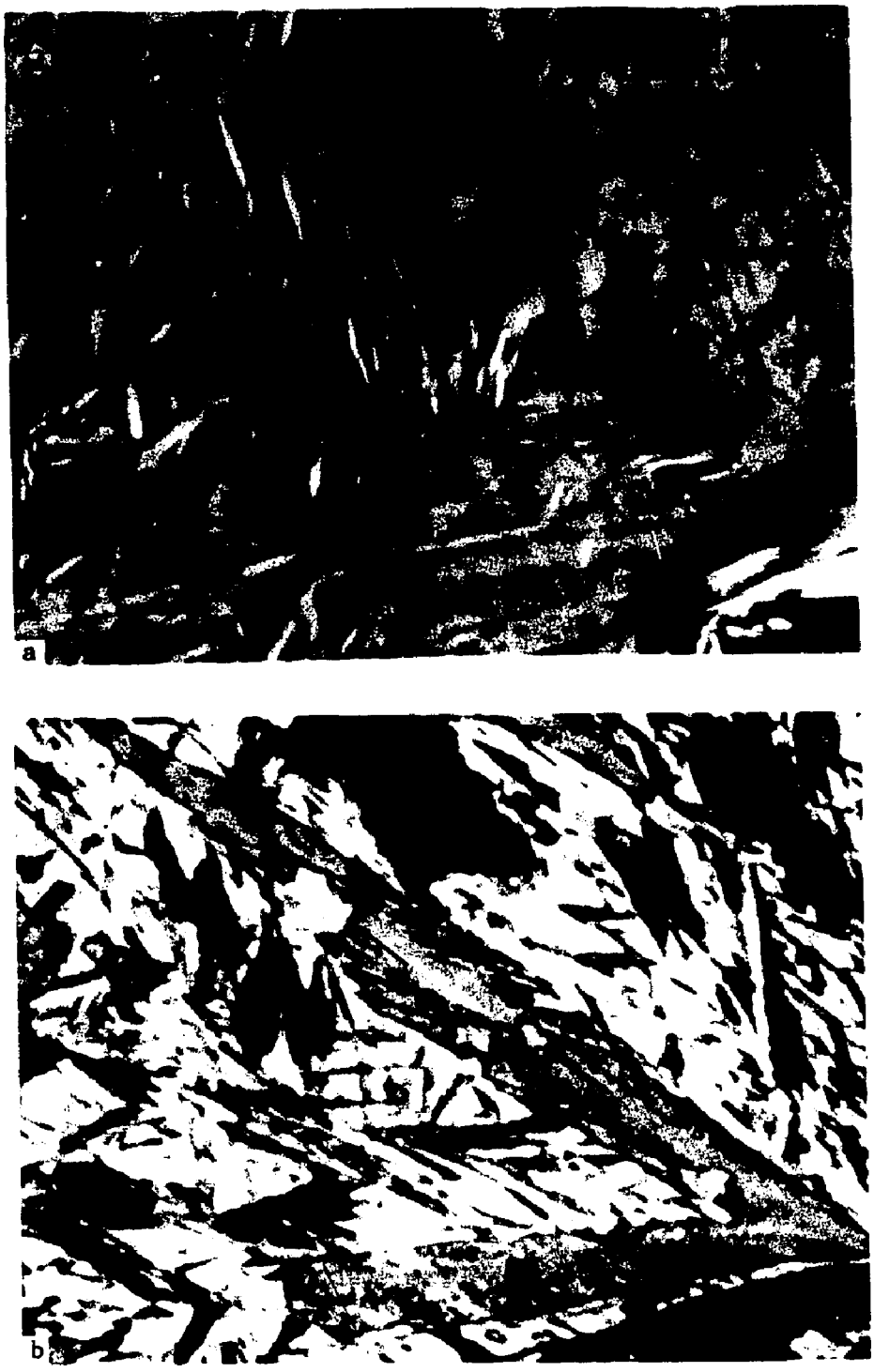

Figure 19 - Surface relief and corresponding structure of the 0.6C alloy partially austenitized at 3°C/s - a) surface relief and b) etched structure. Light photomicrographs. 750X.

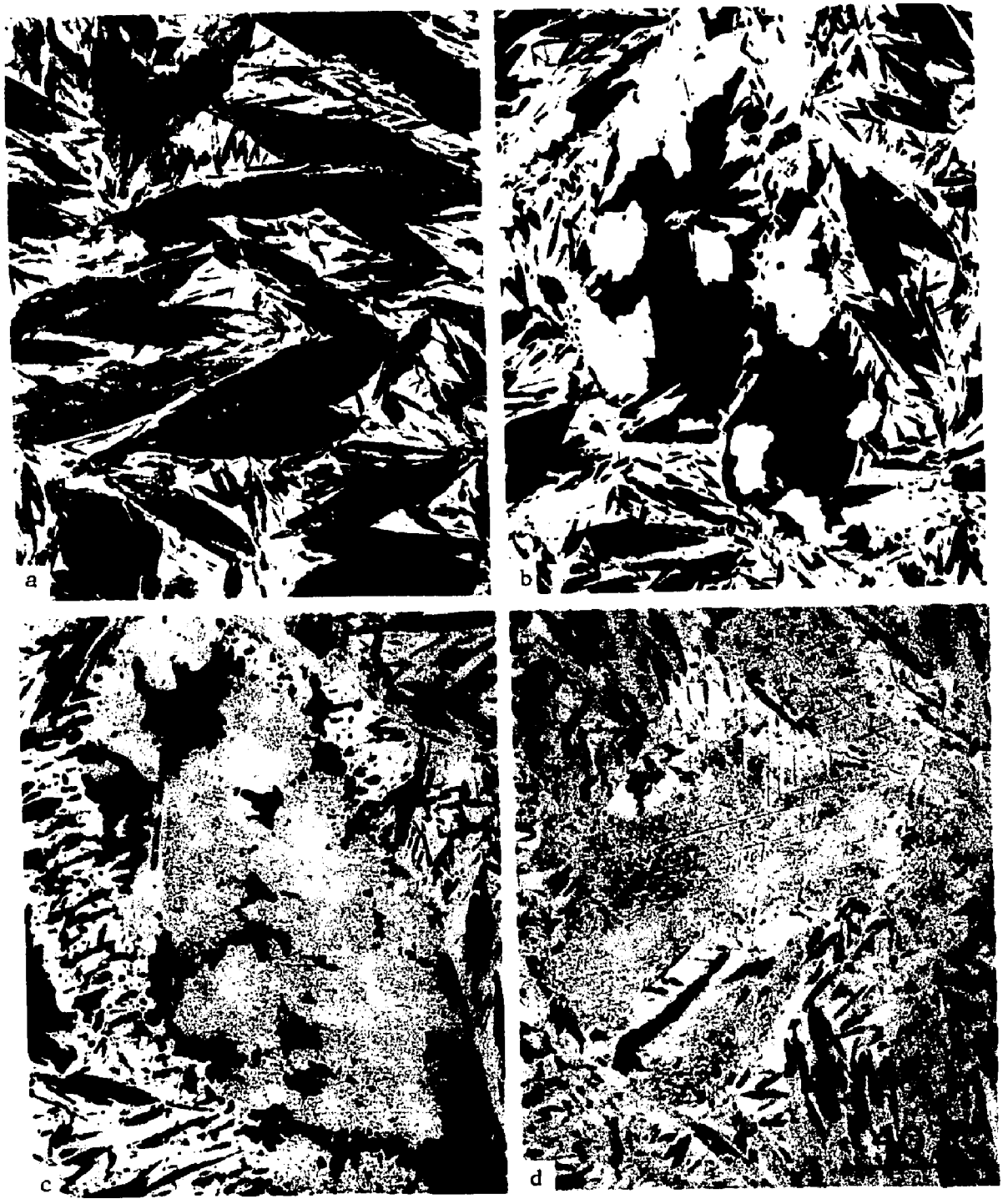

Figure 20 - Microstructure of the 0.6C alloy heated at 3°C/s to - a) 499°C, b) 504°C, c) 509°C, d) 513°C. Light photomicrographs. 532X.

Figure 21 - Microstructures of the 0.6C alloy partially austenitized at - a) 3°C/s and b) 1500°C/s followed by an immediate water quench. Light photomicrographs. 2000X.

Figure 22 - Fine structure of martensite in the 0.3C alloy after cooling to -196°C and storing at room temperature. Transmission electron micrograph. 30,000X.

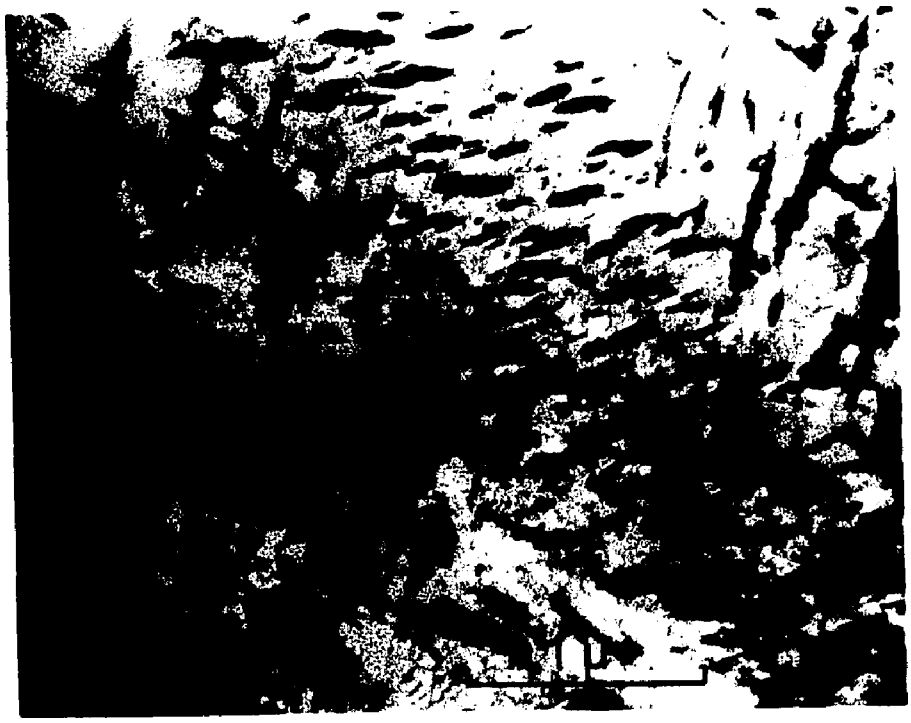

Figure 23 - Carbide distribution in martensite of the 0.3C alloy after heating to 400°C at 3°C/s and cooling to room temperature. Transmission electron micrograph. 30,000X.

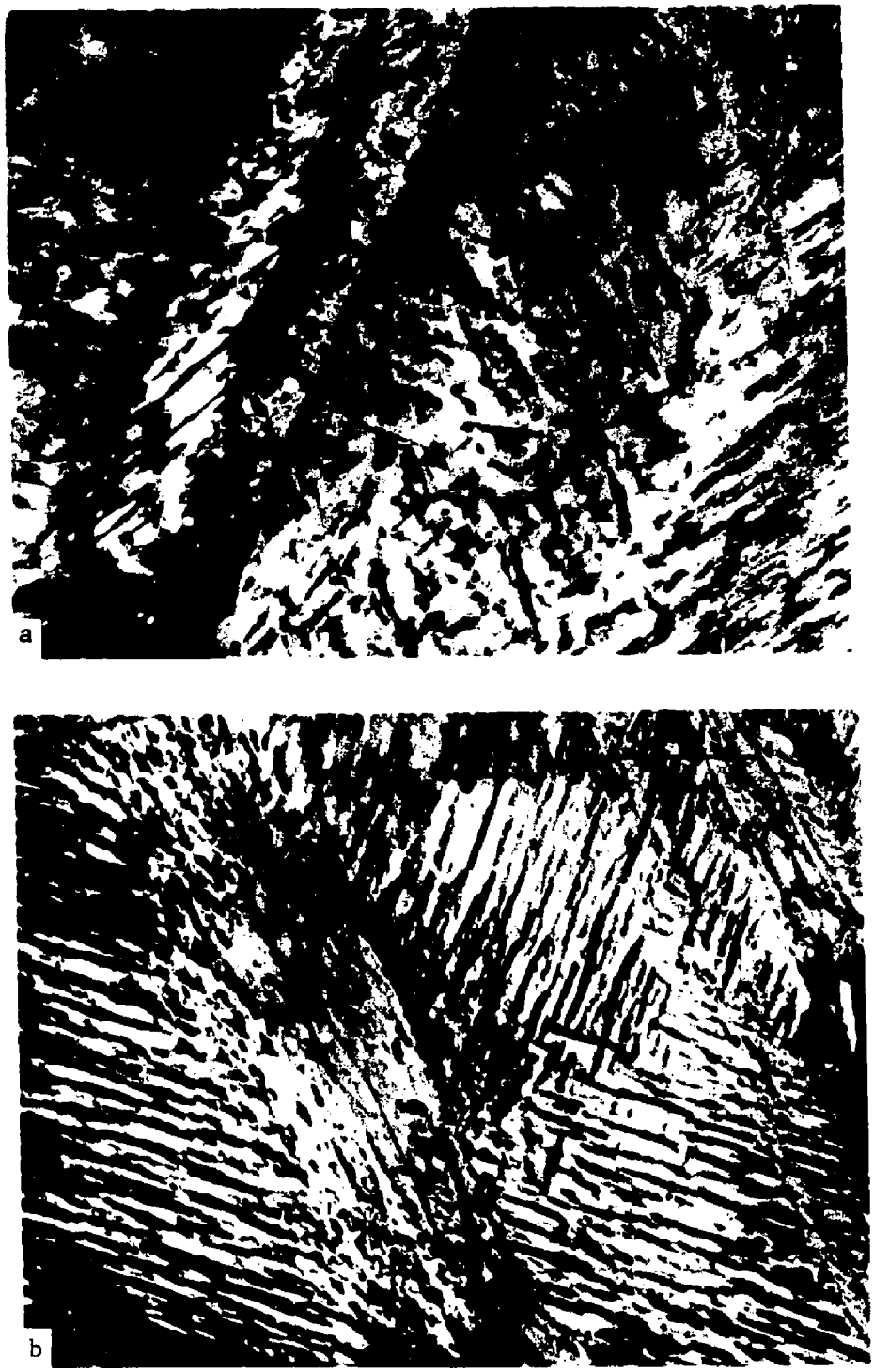

Figure 24 a,b - Carbide distributions in martensite of the 0.3C alloy after heating to 435°C at 1500°C/s followed by an immediate water quench. Transmission electron micrographs. 20,000X.

Figure 25 a,b - Substructure of the 0.3C alloy after partial $\alpha' \rightarrow \gamma$ transformation at 3°C/s. Transmission electron micrographs. 30,000X.

Figure 26 a,b - Acicular austenitic areas in the 0.3C alloy after partial $\alpha' \rightarrow \gamma$ transformation at 1500°C/s. Transmission electron micrographs. 30,000X.

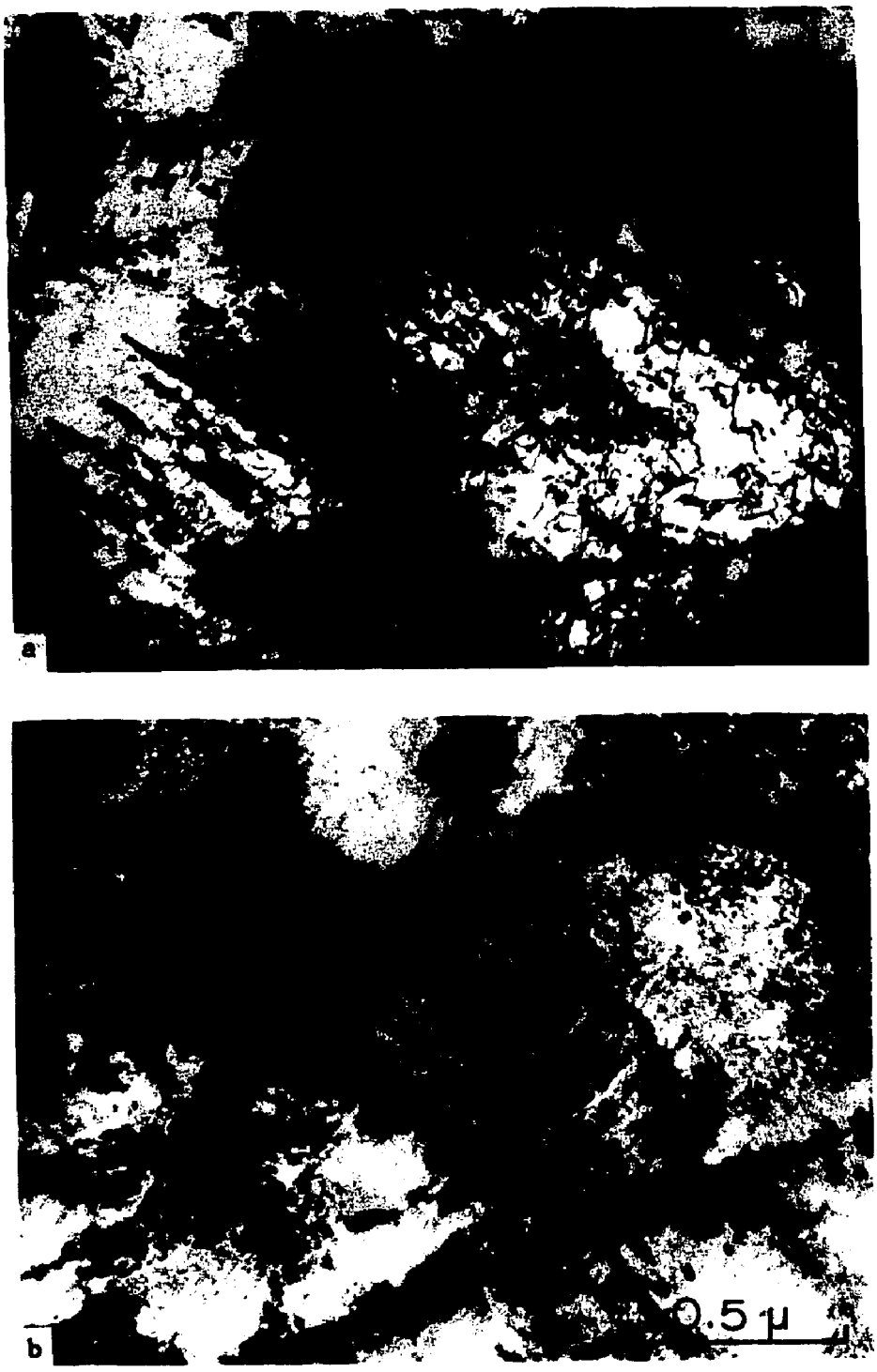

Figure 27 a,b - Austenitic substructure of the 0.3C alloy after $\alpha' \rightarrow \gamma$ transformation at 3°C/s. Transmission electron micrographs. (a) 30,000X - (b) 60,000X.

Figure 28 - Austenitic substructure of the 0.3C alloy after $\alpha' \rightarrow \gamma$ transformation at 1500°C/s. Transmission electron micrograph. 20,000X.

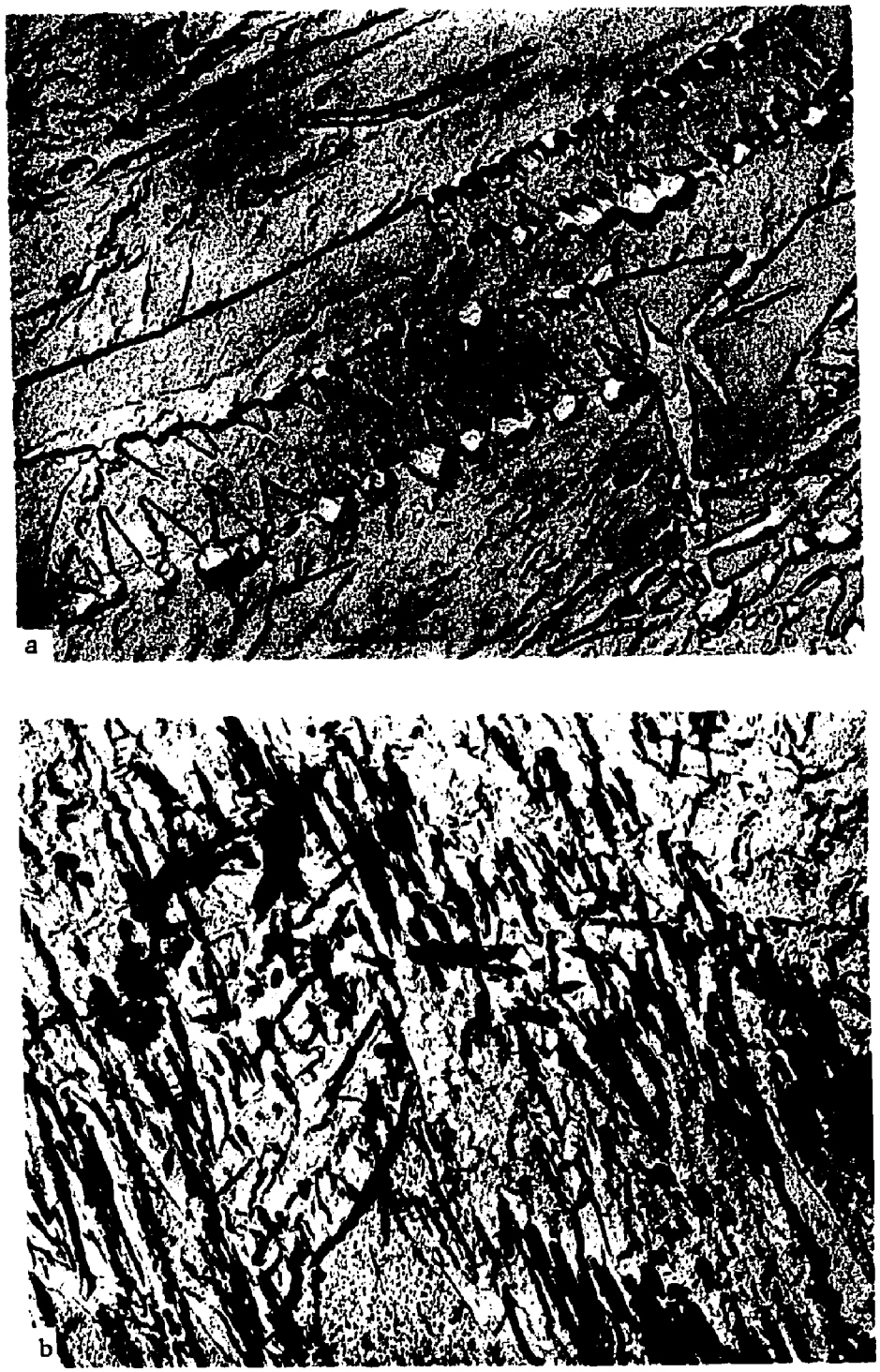

Figure 29 - Carbon extraction replicas prepared from specimens of the 0.3C alloy transformed to austenite at - a) 1500°C/s and b) 3°C/s and cooled to -196°C to form cycled martensite. 15,000X.

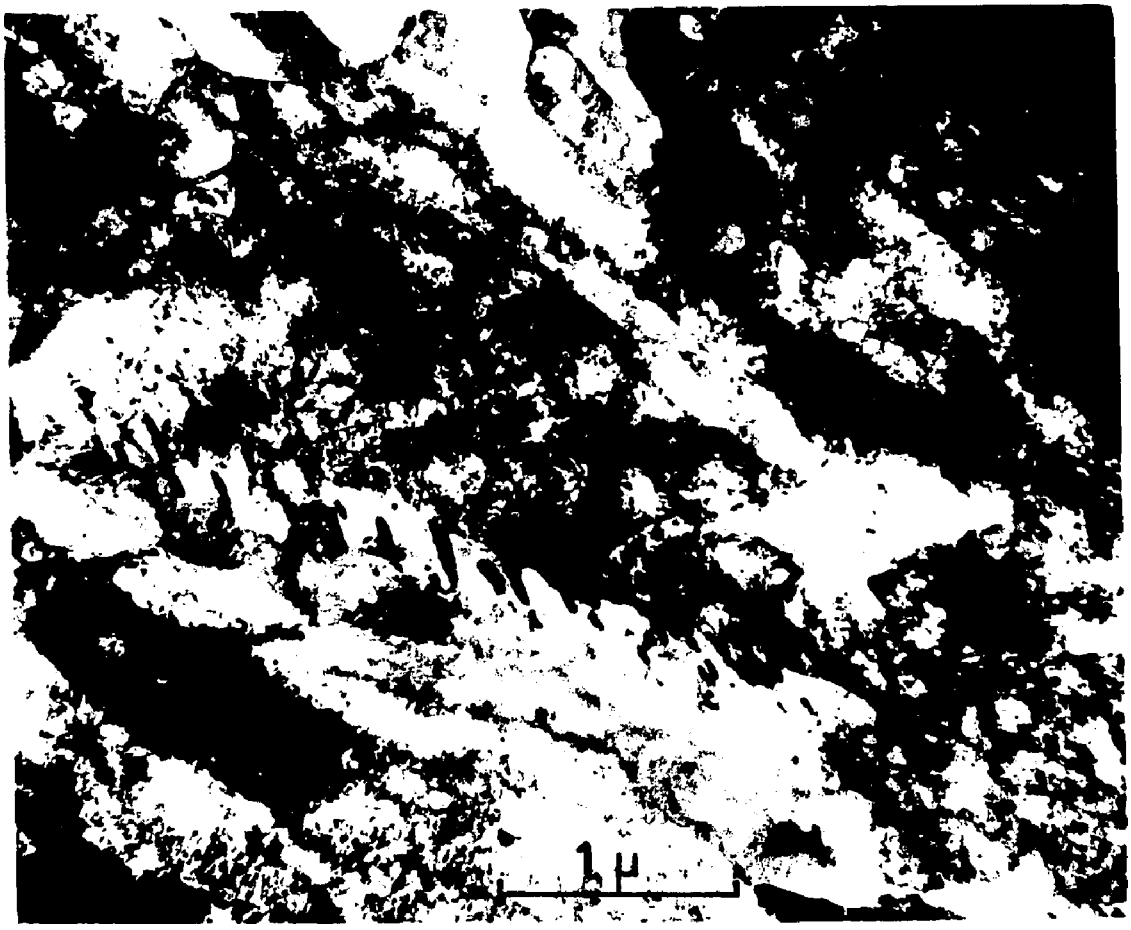

Figure 30 - Austenitic substructure of the 0.3C alloy formed at 1500°C/s from martensite which had been tempered by heating to 400°C at 3°C/s. Transmission electron micrograph. 30,000X.

Figure 31 a,b - Austenitic substructure and carbides in the 0.6C alloy after $\alpha' \rightarrow \gamma$ transformation at 3°C/s. Transmission electron micrographs. (a) 30,000X - (b) 60,000X.

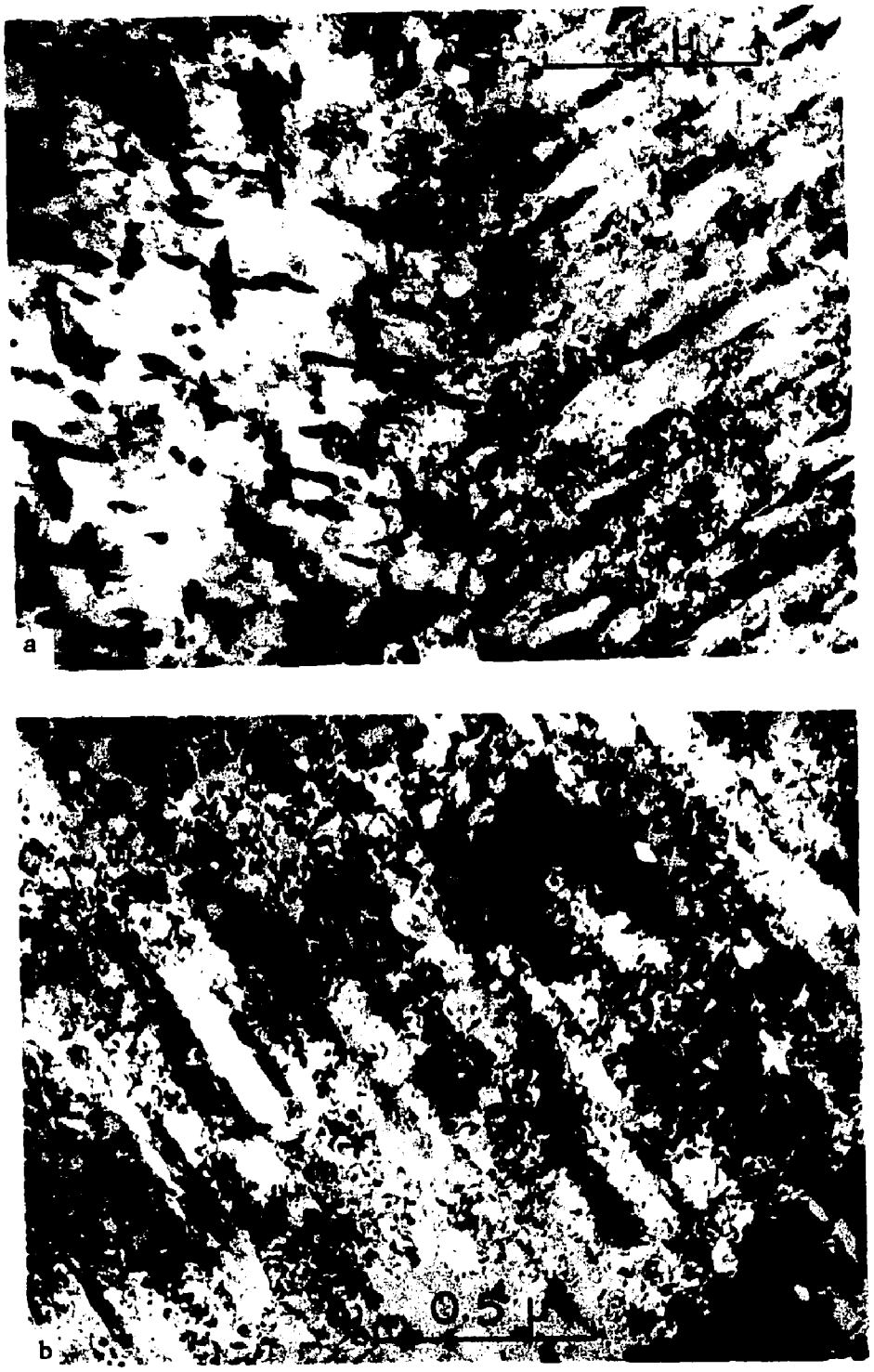

Figure 32 a,b - Austenitic substructure and carbides in the 0.6C alloy after $\alpha' \rightarrow \gamma$ transformation at 1500°C/s. Transmission electron micrographs. (a) 30,000X - (b) 60,000X.

Figure 33 - Austenitic substructure of the 0.05C alloy after $\alpha' \rightarrow \gamma$ transformation at - a) 3°C/s and b) 1500°C/s. Transmission electron micrographs. 30,000X.

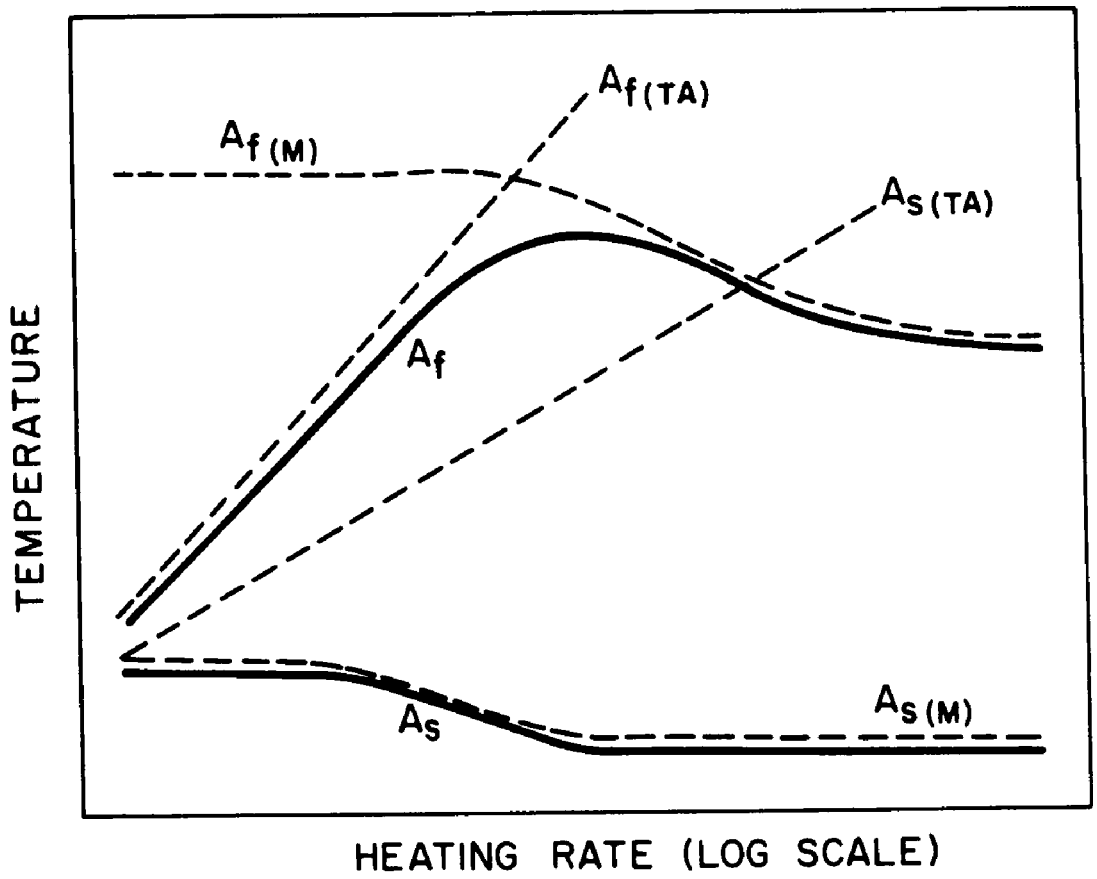

Figure 34 - Schematic representation of a model to explain the general features of A_s and A_f vs. heating rate curves of Fe-Ni-C alloys. Hypothetical transformation temperatures for purely martensitic (M) and pure thermally activated (TA) transformations are shown as dotted lines.

Figure 35 - Microstructure of the 0.6C alloy partially transformed to austenite by heating at 3°C/s - a) to 509°C and immediately quenching and b) to 504°C and hold at 504 ±4°C for 70 sec. Light photomicrographs. 532X.

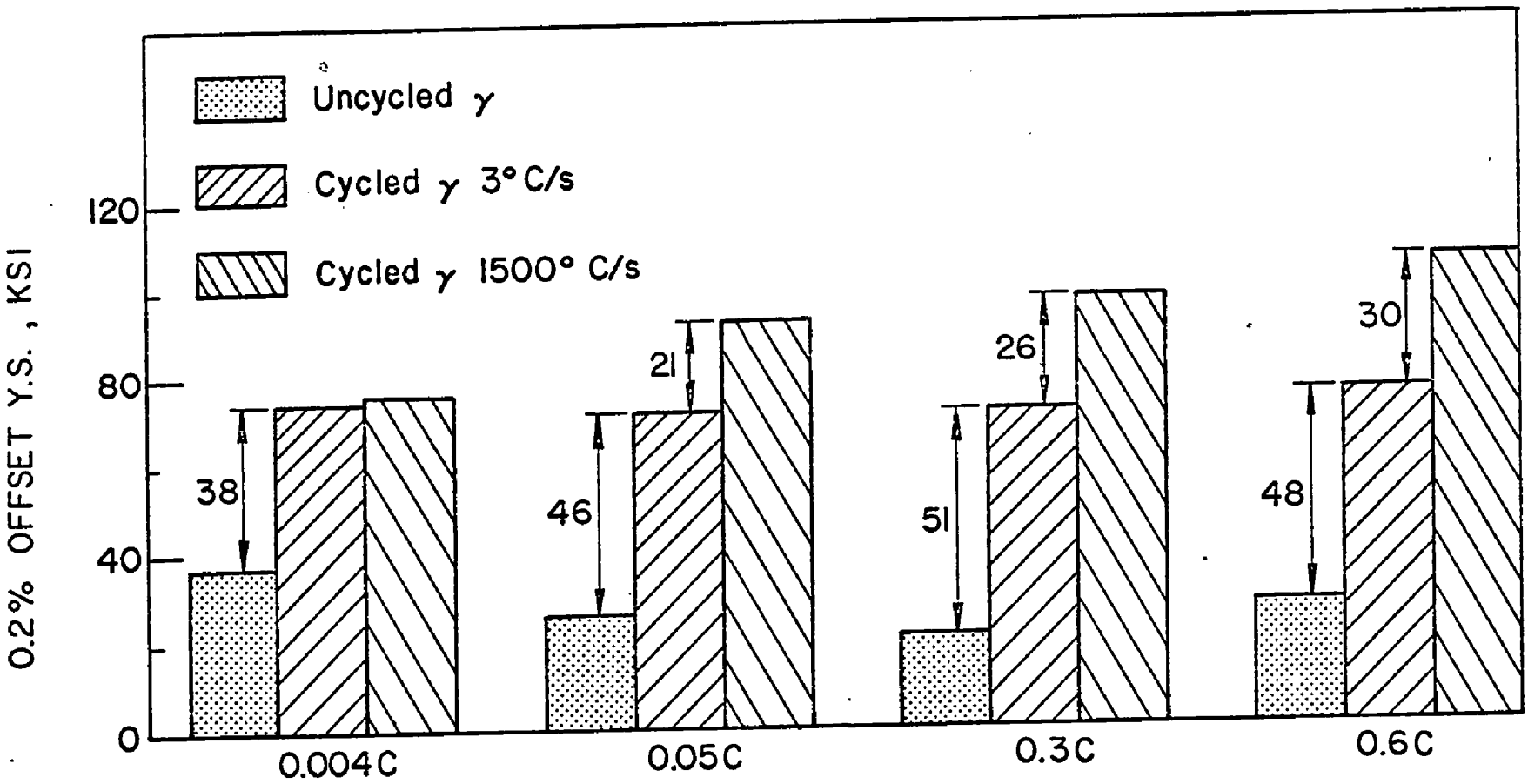

Figure 36 - Bar graph comparing the yield strengths of austenitic specimens after $\alpha' \rightarrow \gamma$ transformation at 3°C/s and 1500°C/s and the yield strengths of uncycled austenitic specimens.

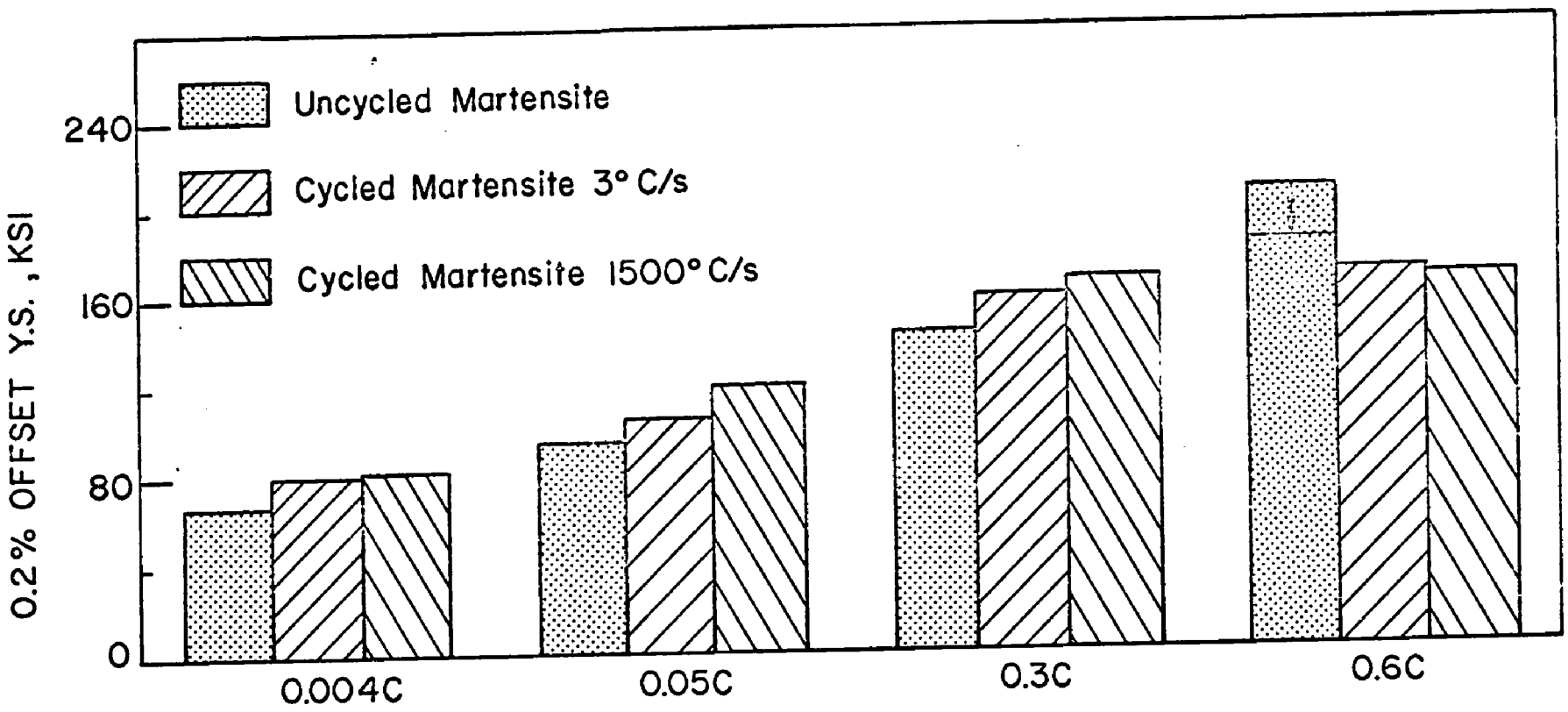

Figure 37 - Bar graph comparing the yield strengths of martensitic specimens after $\alpha' \rightarrow \gamma$ transformation at 3°C/s and 1500°C/s and cooling to -196°C and the yield strength of uncycled martensitic specimens.

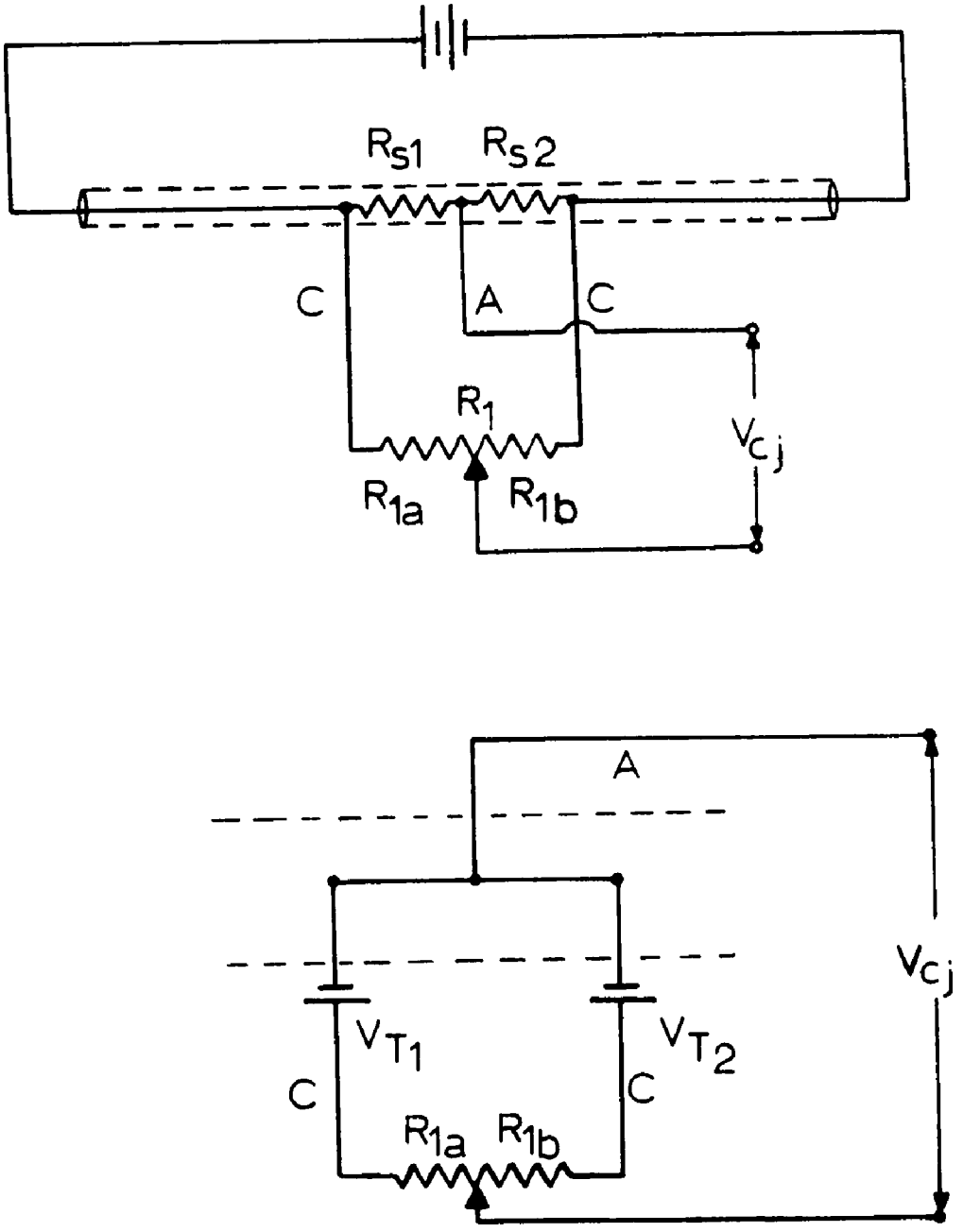

Figure 38 a,b - Simplified schematic representations of the thermotrio circuit illustrating -
a) elimination of non-thermal emf, and
b) relationship of cold junction voltage to the thermal emf's generated by the thermotrio combination.
A ≡ alumel wires C ≡ chromel wires.

REFERENCES

1. J. W. Christian: The Theory of Transformations in Metals and Alloys, Pergamon Press, New York, 1965.

2. L. Kaufman and M. Cohen: The Martensitic Transformation in the Fe-Ni System, Trans. TMS-AIME, 206 (1956), p. 1393-1401.

3. B. Edmondson and T. Ko: Spontaneous Deformation of Austenite During Martensitic Transformations, Acta Met., 2 (1954), p. 235-241.

4. G. Krauss: The Nature of Austenite Produced by the Reverse Martensitic Transformation, Sc.D. Thesis, MIT, 1961.

5. G. Krauss and M. Cohen: Strengthening and Annealing of Austenite Formed by the Reverse Martensitic Transformation, Trans. TMS-AIME, 224 (1962), p. 1212-1221.

6. G. Krauss: Fine Structure of Austenite Produced by the Reverse Martensitic Transformation, Acta Met., 11 (1963), p. 499-509.

7. B. Hyatt and G. Krauss: Cyclic Transformation in Fe-Ni-C Alloys, Trans. ASM, 61 (1968), p. 168-175.

8. C. Apple and G. Krauss: Strengthening of Fe-Ni-V-C Alloy By Cyclic Phase Transformation, Met. Trans., 2 (1971), p. 1785-1791.

9. F. Habrovec, J. Skarek, P. Rys, and J. Kounicky: Rapid Re-Austenitizing of an Fe-Ni-C Alloy, JISI, 205 (1967), p. 861-865.

10. N. K. Nagpaul and D. R. F. West: Strengthening of Austenite in Some High-Alloy Steels by Rapid Re-Austenitizing, JISI, 208 (1970), p. 276-281.

11. H. Kessler and W. Pitsch: Die Martensit-Austenit-Rückumwandlung in einer Eisen-Nickel-Legierung mit 32.5% Ni bei langsamen Aufheizen, Arch. Eisen., 39 (1968), p. 223-231.

12. H. Kessler and W. Pitsch: On the Nature of the Martensite to Austenite Reverse Transformation, Acta Met., 15 (1967), p. 401-405.

13. S. Jana and C. M. Wayman: Martensite-to-FCC Reverse Transformation in an Fe-Ni Alloy, Trans. TMS-AIME, 239 (1967), p. 1187-1193.

14. M. J. Bibby and J. Gordon Parr: The Martensitic Transformation in Pure Iron, JISI, 202 (1964), p. 100-104.

15. A. Gilbert and W. S. Owen: Diffusionless Transformation in Fe-Ni, Fe-Cr, and Fe-Si Alloys, Acta Met., 10 (1962, p. 45-54.

16. W. S. Owen, E. A. Wilson and T. Bell: The Structure and Properties of Quenched Iron Alloys, in High Strength Materials, edited by V. F. Zackay, John Wiley and Sons, Inc., New York, 1965.

17. W. D. Swanson and J. Gordon Parr: Transformations in Fe-Ni Alloys, JISI, 202 (1964), p. 104-106.

18. M. J. Roberts: Effect of Transformation Substructure on the Strength and Toughness of Fe-Mn Alloys, Met. Trans., 1 (1970), p. 3287-3294.

19. H. R. Woehrle, W. R. Clough, and G. A. Ansell: Athermal Stabilization of Austenite, Trans. ASM, 59 (1966), p. 784-803.

20. R. W. Messler, G. S. Ansell, and V. I. Lizunov: The Effect of Quench Rate on the M_s Temperature and the Structure of an Fe-C and an Fe-C-Ni Steel, Trans. ASM, 62 (1969), p. 362-369.

21. E. Hornbogen and W. Meyer: Martensitic Transformation of Solutions with Coherent Particles, Acta Met., 15 (1967), p. 584-586.

22. H. J. Neuhauser and W. Pitsch: A New Observation on the Mechanism of Martensitic Transformations, Acta Met., 19 (1971), p. 337-344.

23. W. L. Haworth and J. Gordon Parr: The Effect of Rapid Heating on the $\alpha \rightarrow \gamma$ Transformation in Iron, Trans. ASM, 58 (1965), p. 477-488.

24. K. J. Albutt and S. Garber: Effect of Heating Rate on the Elevation of the Critical Temperatures of Low-Carbon Mild Steel, JISI, 204 (1966), p. 1217-1222.

25. L. Kaufman and M. Cohen: Thermodynamics and Kinetics of Martensitic Transformations, Progress in Metal Physics, 7 (1958), p. 165-246.

26. J. E. Kittl and C. Rodriguez: The Massive and Martensitic Transformations in Cu-Ga Alloys, Acta Met., 17 (1969), p. 925-928.

27. V. Bharucha, G. A. Mancini, G. W. Powell and J. W. Spretnak: Transformation Kinetics in High Purity Iron and Some Iron Binary Alloys, Trans. TMS-AIME, 221 (1961), p. 498-502.

28. E. Eichen and J. W. Spretnak: The Mechanism of the Allotropic Transformation in High Purity Iron, Trans. ASM, 51 (1959), p. 454-469.

29. H. M. Clark and C. W. Wayman: Surface Relief Effects in Solid-State Phase Transformations, in Phase Transformations, American Society for Metals, Metals Park, Ohio, 1970.

30. P. G. Winchell and M. Cohen: The Strength of Martensite, Trans. ASM, 55 (1962), p. 347-361.

31. Henning, C. D. and Parker, R.: Transient Response of an Intrinsic Thermocouple, Trans. ASME, Journal of Heat Transfer, May 1967, p. 146-152.

32. O. A. Boedtker and P. Duwez: A Delay Time in The Alpha to Gamma Transformation in Iron, USAEC TID-15,069 (1962).

33. J. M. Wallbridge and J. G. Parr: Effect of Rapid Heating on the Mechanical Properties of Low-Carbon Sheet Steel, JISI, 205 (1967), p. 750-755.

34. D. A. Karlyn: Capacitor Discharge Pulse Heating, Trans. ASM, 62 (1969), p. 288-291.

35. A. B. Grenninger: The Martensitic Thermal Arrest in Fe-C Alloys and Plain Carbon Steels, Trans. ASM, 30 (1942), p. 1-26.

36. C. M. Hammond and D. L. Burk: A Simplified Thermal Analysis Technique for Measuring Transformation Temperatures of Steels, Materials Research and Standards, June, 1964, p. 275-278.

37. D. W. Gomersall and J. Gordon Parr: Transformations in Fe-Mn Alloys, JISI, 203 (1965), p. 275-279.

38. Data reported in Reference (25) through private communication.

39. E. Tekin and P. M. Kelly: A Study of the Tempering of Steel Using Transmission Electron Microscopy, in Precipitation From Iron-Base Alloys, edited by G. R. Speich and J. B. Clark, Gordon and Breach Science Publishers, New York, 1965.

40. M. G. H. Wells: An Electron Transmission Study of the Tempering of Martensite in an Fe-Ni-C Alloy, Acta Met., 12 (1964), p. 389-399.

41. K. R. Kinsman: Thermal Stabilization of Austenite in Iron-Nickel-Carbon Alloys, Ph.D. Thesis, Stanford University, 1966.

42. D. A. Karlyn, J. W. Cahn and M. Cohen: The Massive Transformation in Copper-Zinc Alloys, Trans. TMS-AIME, 245 (1969), p. 197-207.

43. K. Hirano, M. Cohen and B. L. Averbach: Diffusion of Nickel in Iron, Acta Met., 9 (1966), p. 440-445.

44. B. S. Lement and M. Cohen: A Dislocation-Attraction Model for the First Stage of Tempering, Acta Met., 4 (1956), p. 469-476.

45. T. B. Massalski: Massive Transformations, in Phase Transformations, American Society for Metals, Metals Park, Ohio, 1970.

46. W. S. Owen and E. A. Wilson: A Note on Massive Structures, in Physical Properties of Martensite and Bainite, ISI Special Report 93, 1965, p. 51-57.

47. G. R. Speich and H. Warlimont: Yield Strength and Transformation Substructure of Low-Carbon Martensite, JISI, 206 (1968), p. 385-392.

48. D. Fahr: Stress and Strain-Induced Martensite and Its Effect on Strength and Ductility of Metastable Austenitic Stainless Steels, Met. Trans., 2 (1971), p. 1883-1892.

49. V. F. Zackay, E. R. Parker, D. Fahr, and R. Busch: The Enhancement of Ductility in High-Strength Steels, Trans. ASM, 60 (1967), p. 252-259.

50. K. J. Irvine, T. Gladman, and F. B. Pickering: The Strength of Austenitic Stainless Steels, JISI, 207 (1969), p. 1017-1028.

51. M. J. Roberts and W. S. Owen: Solid Solution Hardening and Thermally Activated Deformation in Iron-Nickel-Carbon Martensites, JISI, 206 (1968), p. 375-384.

52. A. R. Cox: Effects of Carbide Size and Spacing on Interstitial and Carbide Strengthening in a 0.3 pct. Carbon Steel, JISI, 205 (1967), p. 203-204.

VITA

Charles Arthur Apple was born June 20, 1942 in Jersey Shore, Pa. to Charles A. and Iva B. (Romig) Apple. He attended Parkland High School in Orefield, Pa. and Boca Ciega High School in Gulfport, Fla., from which he graduated in 1960. Mr. Apple served in the United States Marine Corps from 1960 to 1963. He enrolled at Florida State University in September, 1963 and graduated with a B.S. in Engineering Science in April, 1967. In 1965 he married the former Linda Kay Peters of Whitehall, Pa.

From May, 1967, to the present, Mr. Apple has been a research assistant in the Department of Metallurgy and Materials Science at Lehigh University from which he received his M.S. degree in June, 1969. Mr. Apple is a member of the Metallurgical Society of AIME, American Society for Metals, and Sigma Xi.